# Lawrence Berkeley National Laboratory
## LBL Publications


### Title
Allosteric binding properties of a 1,3-alternate thiacalix[4]arene-based receptor having phenylthiourea and 2-pyridylmethyl moieties on opposite faces


### Permalink
https://escholarship.org/uc/item/4p34g3dx



### Journal
New Journal of Chemistry, 45(41)

### ISSN
1144-0546



### Authors
Rahman, Shofiur
Tomiyasu, Hirotsugu
Wang, Chuan-Zeng
et al.



### Publication Date
2021-10-25

### DOI
10.1039/d1nj02991f

Peer reviewed



eScholarship.org Powered by the California Digital Library
University of California

# Allosteric binding properties of a 1,3-*alternate* thiacalix[4]arene-based receptor having phenyl-thiolurea and 2-pyridylmethyl moieties on opposite faces

Shofiur Rahman,[a,c] Hirotsugu Tomiyasu,[a] Chuan-Zeng Wang,[a,b] Paris E. Georghiou,[c*] Abdullah Alodhayb,[d] Cameron L. Carpenter-Warren,[e] Mark R. J. Elsegood,[e] Simon J. Teat,[f] Carl Redshaw,[g] and Takehiko Yamato[a*]

The synthesis of three new heteroditopic receptors (**5a–c**) which are based on thiacalix[4]arenes in the 1,3-*alternate* conformation are reported herein. These new receptors each have two thiourea moieties linking phenyl groups two of which are substituted with electron-withdrawing groups at their *para*-positions, and at the opposite side of the thiacalix[4]arene cavity, with two 2-pyridylmethyl groups. One example (**5a**) was also characterized by X-ray crystallography. A limited $^1$H-NMR and Uv-vis anion complexation study was conducted. DFT computational determinations indicated that **5c** which has the strong electron–withdrawing $NO_2$ groups had the most effective recognition ability towards the selected anions. The binding of $Ag^+$ at the 2-pyridyl moieties and the binding of the anions at the two thiourea NH groups of the *p*-substituted phenylthioureido moieties, respectively, was also investigated. The appearance of a positive allosteric effect with receptor **5b** was also found using $^1$H-NMR titration experiments.

## Introduction

Calix[*n*]arenes, which are macrocyclic compounds comprised of alternating numbers [*n* = 3–8] of phenolic groups typically linked via $-CH_2-$ groups, have proven to be versatile and useful building blocks for a variety of applications, especially in host-guest chemistry. This is due to the fact that they are easily synthesized and can be modified with a wide range of functional groups which can be fine-tuned for a variety of applications.[1] One of the most widely explored areas of calix[*n*]arene chemistry has been in the development of sensitive and selective ionophoric receptors for cations, and also anions.[1] Included in the class of calix[*n*]arenes are the thiacalix[4]arene analogues, in which four alternating phenolic groups are linked via divalent sulfur atoms.[2] While not as extensively studied as the "classical" calix[4]arenes they nevertheless have shown similarities in their host-guest chemistry as chemosensors or receptors for metal cations, since they can also be relatively easily functionalized.[3] As well, thiacalix[4]arenes can also adopt the various conformations that are characteristic of calix[4]arenes. Our own work in this area has led us to report on new thiacalix[4]arenes which are locked in 1,3-*alternate* conformations and which are functionalized with two urea moieties and two benzyl groups on opposite sides.[4]

An area of great important and interest concerns allosteric effects and regulation[5] involving ions in biological systems. Several different types of artificial systems including calix[4]arenes have been shown to be suitable for the study of allosteric effects in host-guest interactions involving metal cations. In our own work, we have been able to demonstrate allosteric effects with thiacalix[4]arene derivatives resulting from their interactions with alkali metal cations.[6–8]

Anions are also important for biological processes, involving DNA and as enzyme substrates, for example. There is therefore much interest in also developing artificial anion-selective sensors or receptors. However, since commonly encountered anions have varied shapes as compared with those of metal cations, the design of anion receptors can be more challenging.[9] Thus, for example, apart from halide anions which are spherical, anions can also be trigonal such as *e.g.* acetate ($AcO^-$) or benzoate ions; or tetrahedral, such as e.g. dihydrogenphosphate ($H_2PO_4^-$) and perchlorate ions, to name just a few. A desired feature of sensitive anion chemosensors is that they also be colorimetric, and many anion chemosensors have been reported having chromogenic signaling moieties such as anthraquinone, benzenediimide, and *p*-nitrophenylazo groups which have been incorporated in a variety of structural scaffolds which contain urea groups.[10–12] These have proven to be efficient naked–eye colorimetric detectors for various anions since hydrogen-bonding interactions can occur between them and the urea NH

protons. However, there are relatively few reports of colorimetric anion chemosensors based on calix[4]arene[12(l),12(p)] or thiacalix[4]arene scaffolds.[13,14] Recently, J. Schatz reported two highly selective naked-eye anion sensors based on *cone* conformation *tetrakis*urea- and a *tetrakis*thioureidocalix[4]-arene.[15]

We now report on our further studies, with heteroditopic thiacalix[4]arenes (**5a**–**c**) which were derived from tetra-*p*-*tert*-butyl thiacalix[4]arene (**1**), and are in 1,3-*alternate* conformations. These new thiacalix[4]arene-based receptors are di-substituted on one side with thiourea moieties linked to either unsubstituted phenyl groups (**5a**), or electron-withdrawing *p*-fluorophenyl (**5b**) or *p*-nitrophenyl (**5b**) groups. At the opposite 1,3 position of the thiacalix[4]arene cavity are two 2-pyridylmethyl groups. We herein demonstrate that heteroditopic receptor **5b** undergoes complexation with either or both $F^-$ anions and $Ag^+$ ions at its opposite sides, with an effective and positive allosteric effect. This receptor molecule can also serve as a sensitive colorimetric fluoride anion sensor.

## Results and discussions

### *Synthesis*

*O*-Alkylation of **1**[16] with 2 mol equiv. of 2-bromoacetamide in the presence of $Na_2CO_3$ using a reported procedure[17] afforded the 1,3-di-*O*-substitution product, *distal*-**2**, in 64 % yield as the major product, with no other possible isomers being observed. The reaction of **2** with 2-(chloromethyl)pyridine in acetone in the presence of $Cs_2CO_3$ formed 1,3-*alternate*-**3** in 52 % yield. Reduction of **3** with $BH_3$ under THF reflux conditions afforded 1,3-*alternate*-**4** in 82% yield. Condensation reactions of **4** in $CH_2Cl_2$ with 2.2 equivalents of the appropriate phenylthioisocyanate furnished the corresponding thiourea receptors **5a**–**c** in good to excellent yields (Scheme 1). The $^1$H–NMR spectra of **5a**–**c** in $CDCl_3$–DMSO-$d_6$ (10:1, v/v) all exhibited the characteristics of 1,3-*alternate* conformations. The spectra showed two 18-proton singlets for the *tert*-butyl protons, one 4-proton singlet for the –O***CH*****$_2$**CO– protons, two 4-proton triplets for the –O***CH*****$_2$*****CH*****$_2$**– protons, two 4-proton singlets for the aromatic protons and two 2-proton singlets for the four urea NH

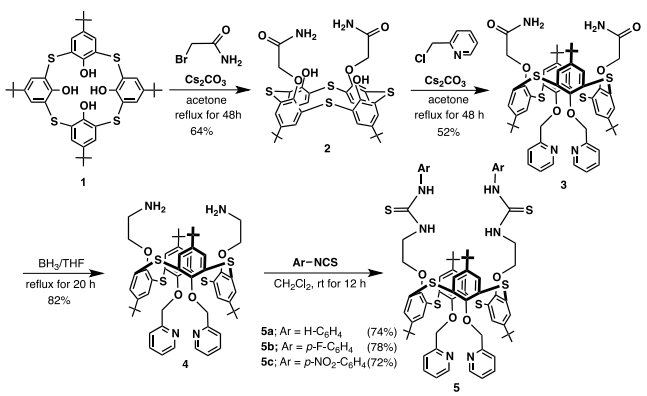


**Scheme 1** Synthesis of receptors 1,3-*alternate*-**5a**–**c**.

The structure of **5a** was verified by a single-crystal X-ray analysis (Fig. 1 and Figs. S13–S17). **5a** was crystallized by slow evaporation from a mixture of $CHCl_3$–$CH_3CN$ (1:1, v/v) in the presence of one equiv. of tetra-*n*-butylammonium chloride (TBACl) . The asymmetric unit comprises two different calixarene moieties, one having the molecular formula for **5a** of $C_{70}H_{78}N_6O_4S_6$ and with a $Cl^-$ ion and the other, **6**, whose molecular formula is $C_{57}H_{67}N_4O_4S_4^+$, with a $Cl^-$ion, and a $CHCl_3$ solvent molecule of crystallization. The charge on the $Cl^-$ anion is stabilised by charge-assisted hydrogen bonding from a fairly rare $[–NH–CH–NH–]^+$ moiety. This group has a delocalized positive charge on the second, modified, thiacalixarene molecule in the asymmetric unit (Fig. 2 and Figs. S13–S14). From the N–C bond lengths, it is clear that individually they are neither single nor double bonds but share the delocalized positive charge across both bonds. The asymmetry of the bond lengths is a result of H(5) interacting with the $Cl^-$ anion, thus lengthening the N(3A)–H(5) bond and, as a result, shortening the adjacent N–C bond (Fig. 2). This cationic moiety is demonstrating an ability to capture chloride ions. There are currently 17 structures in the CSD which exhibit the same functional group (*e.g.* XANFIC, RURWUY, MAJSEV),[18] in which both C–N bonds are roughly 1.30 Å, with any asymmetry in the two bond lengths being attributed to different substituents on either side of this functional group.

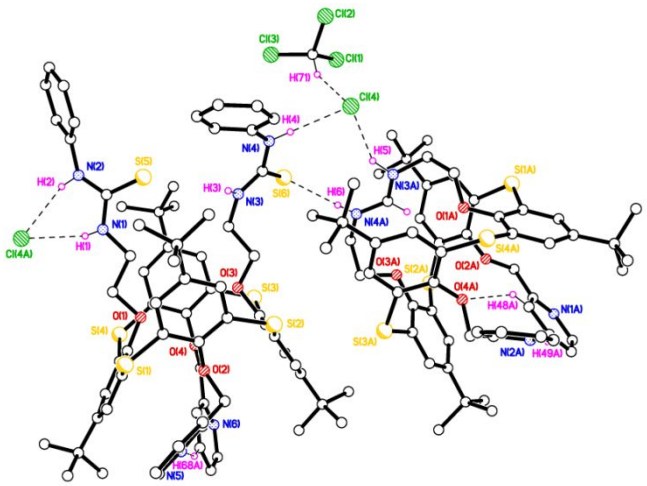


**Fig. 1** X–ray crystal structure of **5a** (*left hand side*) and **6**. The asymmetric unit shows an intermolecular S···H–N hydrogen bond between the two different thiacalixarenes and the N–H···$Cl^-$ interactions between each thiacalixarene and the $Cl(4)^-$ anion; Cl(4A) is a symmetry equivalent. Minor disorder components and H atoms not involved in H-bonding are omitted for clarity.

One of the thiacalixarene molecules in the asymmetric unit, both of which are in 1,3-*alternate* conformations, shows weaker intramolecular C–H···N hydrogen bonding between the opposing pyridine rings (Fig. S15). The other thiacalixarene in the asymmetric unit also shows intramolecular hydrogen between the opposing pyridine groups in addition to the charge-assisted N–H···$Cl^-$ hydrogen bonding (Figs. S16–S17). There is also an intermolecular S···H–N hydrogen bond between the two thiacalixarenes (Fig. 1 and Figs. S16–S17). The three-dimentional cavity within receptor **5a** is large enough to accommodate a metal cation between the opposing 2-pyridyl side-arms. The precise mechanism for the formation of the unexpected cationic compound **6** can only be conjectured from the available data. However, it can be envisioned that under the crystallization conditions

employed with the unambiguously pure sample of **5a** that the TBACl facilitated either a concerted, or step-wise phenylisothiocyanates elimination-intramolecular nucleophilic substitution-coupling reaction with a molecule of $CHCl_3$ (Scheme S1).[19]

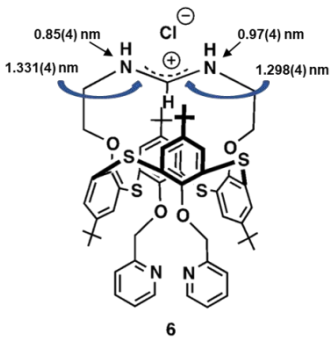


**Fig. 2** Structure of **6** showing the bond lengths (Å) of the $[–NH–CH–NH–]^+$ moiety with it's delocalized positive charge.

### *Binding studies*

*$^1$H- NMR-spectroscopy*:

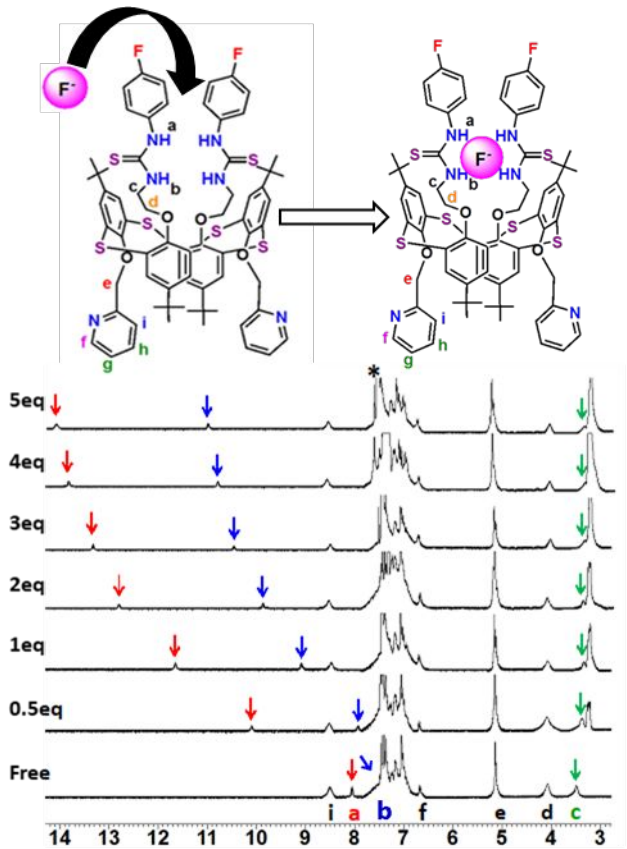


**Fig. 3**. *Top*: Binding mode of **5b** upon addition of $F^-$, and *below*: partial $^1$H-NMR (300 MHz at 298 K) spectra in $CDCl_3$–DMSO-$d_6$ (10:1, v/v).

The anion binding properties of **5a–c** in the presence of $F^-$ as its TBA salt, in a $CD_3CN$ solvent solution, were investigated by means of $^1$H–NMR spectroscopic titration experiments. As shown in Fig. 3, for the complexation of $F^-$ with **5b**, for example, the signals for the $NH_a$ protons (red) progressively shifted downfield by 5.99 ppm (from $\delta$ = 8.06 to 14.05 ppm) and the signals for the $NH_b$ protons (blue) progressively shifted downfield by 3.62 ppm (from $\delta$ = 7.34 to 11.02 ppm), until five equiv. of $F^-$ were added (Fig. S18). These results are strongly suggestive of $F^-$ recognition by the receptor **5b** *via* hydrogen–bonding interactions between $F^-$ and the N–H protons. On the other hand, the methylene protons adjacent to the $NH_b$ moiety (green) are shifted slightly upfield. A similar $^1$H–NMR spectroscopic titration experiment with receptor **5a** in the same solvent mixture (Fig. S19) showed that addition of $F^-$ also resulted in clear downfield shifts of the $^1$H–NMR signals of the $NH_a$ protons. Moreover, the addition of $F^-$ (1.0 equiv.) to solutions of receptor **5c** in the same solvent during the titration experiments resulted in the disappearance of the signals for the thiourea $NH_a$ and $NH_b$ protons (Fig. S20). These results also indicate that strong interactions between these anions and the thiourea NH groups in the receptor **5c** occur and that the kinetics of these anion exchanges are on the NMR time scale. The results obtained from the $^1$H–NMR spectroscopic titration experiments clearly suggest that anion recognition by the receptors is *via* hydrogen-bonding interactions between the anion and the NH protons and is consistent with previously reported studies by us and others, with urea moiety-containing receptor molecules. The apparent binding or association constant ($K_a$) values were 250 and 477 $M^{-1}$, respectively from 1:1 global fit analyses[20a,b] of the chemical shift changes seen in the single titration experiments for the $NH_a$ and $NH_b$ protons of receptors **5a** and **5b** with $F^-$ (Figs. S18–19). These values are of the same order of magnitude as those noted by Schatz and coworkers[15] in their study. The $K_a$ value for **5b**, which has the electron-withdrawing F substituents on the phenylureido moieties, is nearly twice that of **5a**. Thus, the $K_a$ values are influenced by the presence of an electron-withdrawing group at the *para* position of the phenylureido moieties since it further increases the known stronger acidity of the thiourea protons (relative to those of urea protons[21]) and hence enhances the anion-binding ability through hydrogen-bonding interactions.

$^1$H–NMR titration experiments of **5b** with $AgSO_3CF_3$ were conducted in $CDCl_3$–DMSO-$d_6$ (Fig. 4). Addition of a molar equiv. of $AgSO_3CF_3$ causes an upfield shift ($\Delta\delta$ = 0.25 ppm) from $\delta$ = 5.13 to 4.88 ppm for the methylene –O$CH_2$Py protons of **5b** (Fig. 4g). Also, the pyridine protons ($H_{f-i}$) all show downfield shifts, indicating that the $Ag^+$ is bound to the phenolic oxygens and the nitrogen atoms of the pyridine appendage. The downfield chemical shift change of the $H_f$-pyridyl protons adjacent to the nitrogen is by a larger amount ($\Delta\delta$= –0.39 ppm, from $\delta$ = 8.50 to 8.89 ppm) than those of the other pyridyl protons. Further spectral changes in the presence of an excess of $AgSO_3CF_3$ were not detectable, which supports the exclusive formation of a 1:1 **5b**⊃$Ag^+$ complex. From these observations, it is clear that for the complexation of **5b** with $Ag^+$, the pyridine nitrogens turn inward to bind with the $Ag^+$ within the cavity of the receptor, as depicted in Fig. 4. On the other hand, the chemical shifts of the methylene protons in the –O$CH_2$Py moieties move in the opposite direction due to the ring current effect of the benzene moieties. The Job plot[22] for the titration of **5b** with $Ag^+$ exhibited a 1:1 stoichiometry. The different sites of complexation for the anions and $Ag^+$ suggested the potential for an effective positive or

negative allosteric effect between receptor **5b**⊃$F^-$ and $Ag^+$. Thus, a $^1$H-NMR titration experiment was undertaken to determine this hypothesis.

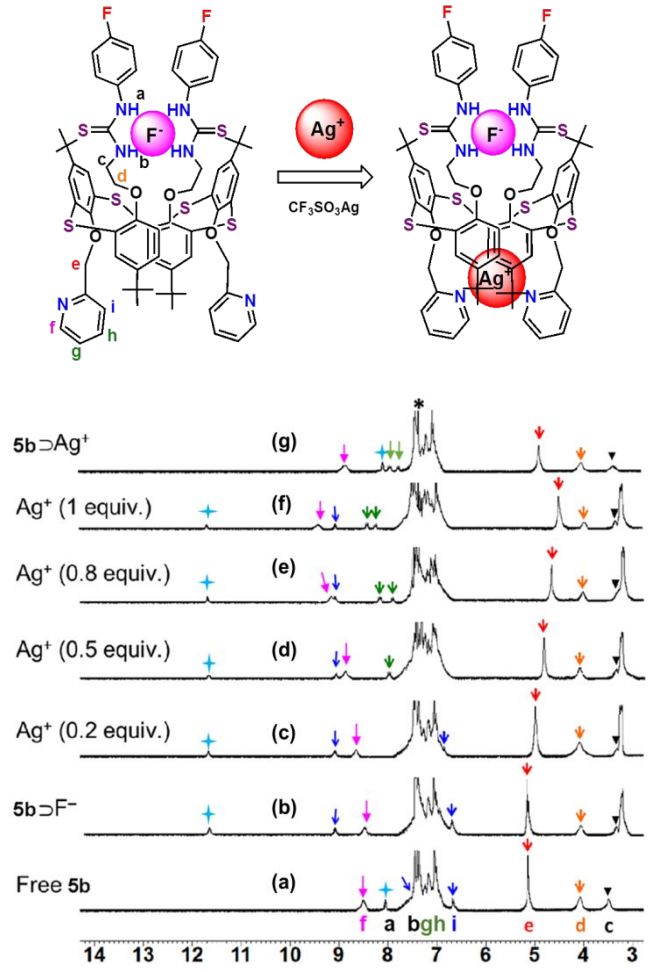


**Fig. 4.** Binding mode of [**5b**⊃$F^-$] upon addition of $Ag^+$ and partial $^1$H-NMR (300 MHz at 298 K) spectra in $CDCl_3$–DMSO-$d_6$ (10:1, v/v) of **5b** showing the positive allosteric behaviour of receptor **5b** with $F^-$ and $Ag^+$ ions: (a) free **5b**; (b) **5b**⊃$Bu_4NF$ (1:1); (c) $AgSO_3CF_3$ (0.20 equiv.)⊂[**5b**⊃$F^-$]; (d) $AgSO_3CF_3$ (0.50 equiv.)⊂[**5b**⊃$F^-$]; (e) $AgSO_3CF_3$ (0.80 equiv.)⊂[**5b**⊃$F^-$]; (f) $AgSO_3CF_3$ (1.0 equiv.)⊂[**5b**⊃$F^-$]; (g) $AgSO_3CF_3$⊂**5b** (1:1). *Denotes the solvent peak.

Figs. 4c–f show that as $Ag^+$ is added to the solution of the 1:1 **5b**⊃$F^-$ complex, a downfield chemical shift of the pyridine protons and a corresponding upfield chemical shift of the –O$CH_2$Py methylene protons occurs. On the other hand, the chemical shifts for the thiourea amido protons did not change. The addition of 1.0 equiv. of $AgSO_3CF_3$ to the 1:1 **5b**⊃$F^-$ complex causes a larger upfield shift for the –O$CH_2$Py methylene protons ($\delta\Delta$ = 0.79 ppm, from $\delta$ = 5.13 to 4.56 ppm) than that previously seen when a molar equivalent of $Ag^+$ was added to **5b** on its own ($\delta\Delta$ = 0.25 ppm, from $\delta$ = 5.13 to 4.88 ppm)) itself (Fig. 4g). Moreover, a larger downfield shift was observed for the pyridyl $H_f$ proton ($\delta\Delta$ = 0.89 ppm, $\delta$ = 8.50 to 9.39 ppm) than that previously seen with **5b** on its own ($\delta\Delta$ = 0.39 ppm, from $\delta$ = 8.50 to 8.89). These observations suggest that a stronger binding ability occurs for the preformed **5b**⊃$F^-$ complex with $Ag^+$ than for **5b** alone.

These results also support the formation of a heteroditopic dinuclear complex such as $Ag^+$⊂[**5b**⊃$F^-$] as shown in Fig. 4, and that a positive allosteric effect of receptor **5b** towards $Ag^+$ in the presence of $F^-$ occurs. Presumably, this occurs as a result of the anion-electrostatic interactions with the N-H atoms of the 1,3-thioureido pair, resulting in a conformational change of the flexible thiacalix[4]arene. This can allow for the $Ag^+$ complexation within the cavity and complexed with by the pyridinium nitrogen atoms. These obswevations are also supported by the DFT computational study.

*UV-vis spectroscopy*

A UV–vis spectroscopic binding study of **5a–c** with $F^-$, $Cl^-$, $AcO^-$, and $H_2PO_4^-$ ions was conducted in $CH_2Cl_2$. Upon successive additions of aliqots of $F^-$ (0–50 μM) to the $CH_2Cl_2$–DMSO solution of **5c** (Fig. 5), a gradual decrease in the absorption of the band at 305 nm with a simultaneous increase in the absorption centred at 355 nm with a clear isosbestic point at 340 nm can be seen. Similar UV–vis spectra can be seen for the titration of $AcO^-$ with **5c** (Fig. S21). In the case of **5c** upon addition of 5 equiv. $F^-$ the colour of the solution changed, and was easily visible, from colourless to yellow. This indicates that a quinoidal structure was most likely formed by the deprotonation of the thiourea NH groups in the 4–nitrophenylureido moiety. The Job's plot (Fig. S22) also shows 1:1 stoichiometry for the binding between receptor **5b** and $F^-$ in the UV-vis titration.

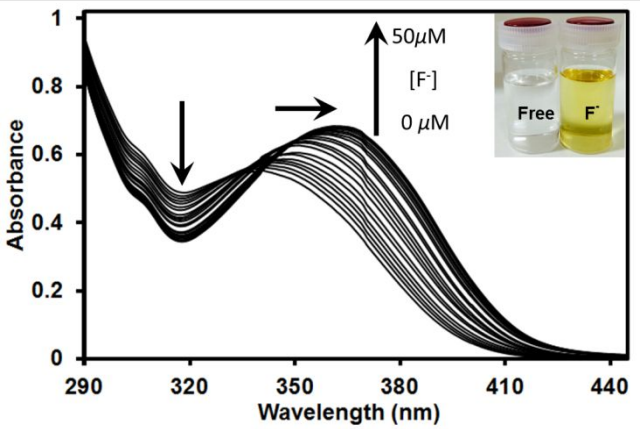


**Fig. 5.** UV–vis absorption spectra of receptor **5c** (2.5 μM) upon the addition of $Bu_4NF$ (0–50 μM) in $CH_2Cl_2$–DMSO (10:1, v/v). *Inset*: The solution color of receptor **5c** in the absence and presence of 5 equivalents of $F^-$ ion.

*DFT computational study*

A DFT computational study was undertaken to determine the binding site of the anions tested with receptors **5a–c**. The individual structures were fully geometry-optimized in the gas-phase as well as with solvent continuum corrections for dichloromethane (DCM), and also for dimethyl sulfoxide (DMSO), using *Gaussian 16*[23] at the B3LYP level of DFT and the LANL2DZ basis set.[24] Significant changes were observed for the distances between the two thiourea NH moieties in each of the receptors in their anion complexes. The conformational changes for the 1:1 complex of **5b** with $F^-$, for example, can be seen in Fig. 6b (see also Table S1, and Figs. S23–S25). The hydrogen-bonding distances between the $F^-$ ion and each of

the thiourea NH protons ($NH_a\cdots NH_{a'}$ and $NH_b\cdots NH_{b'}$) on the two *p*-fluorophenylureido moieties decrease from 8.783 to 2.530 (Å) and from 8.379 to 3.251 (Å), respectively. The interaction energies (*ΔIE*) for the receptor (*R*)**:** anion (*X*) complexes i.e. $R \supset F^-$, $R \supset Cl^-$, $R \supset AcO^-$, $R \supset H_2PO_4^-$, $R \supset Ag^+$; $Ag^+ \supset R \subset F^-$ were calculated by using the following equations:

$$\Delta IE_{[R\supset Ag^+]} = E_{[R\supset Ag^+]} - (E_{[R]} + E_{[Ag^+]}) \quad (1)$$

$$\Delta IE_{[R\supset X^-]} = E_{[R\supset X^-]} - (E_{[R]} + E_{[X^-]}) \quad (2)$$

$$\Delta IE_{[Ag^+\supset R\supset X^-]} = E_{[Ag^+\supset R\supset X^-]} - ((E_{[R]} + E_{[Ag+]}) + E_{[X^-]}) \quad (3)$$

*Note*: *X*= $F^-$, $Cl^-$, $AcO^-$, and $H_2PO_4^-$

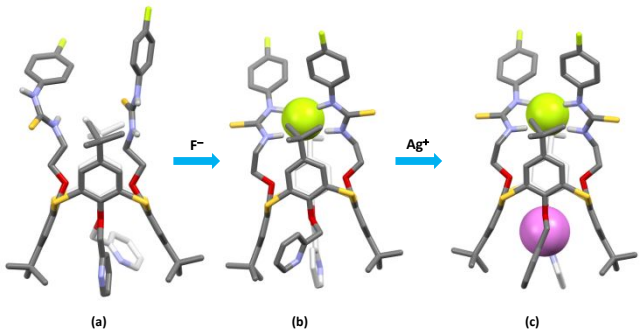


**Fig. 6.** Geometry-optimized (ball-and-stick) structures (in DCM) of: (a): Free receptor **5b**; (b): **5b**⊃$F^-$ and (c): $Ag^+$⊂[**5b**⊃$F^-$]. Colour code: $F^-$ = green, nitrogen = blue, sulfur = yellow, oxygen = red, carbon = grey, hydrogen = white and $Ag^+$ = violet.

The DFT data in Table 1 shows that the trend for the interaction energies for **5b** are in following order: $F^- > AcO^- > H_2PO_4^- > Cl^-$. It should be recognized however, that the DFT study could not exactly match the experimental conditions in which a mixed solvent system was used. Furthermore, the strong base anions ($F^-$ and $AcO^-$) likely resulted in further proton extaction from the receptor molecules, which could also not be adequately modeled in the DFT calculations. The best correlation could be observed with the solvent correction with DCM (see also Table S1).

**Table 1**. Calculated interaction energies (*ΔIE*) for receptors **5a**–**c** with anions.

| | | *ΔIE* (kJ mol$^{-1}$) in DCM solvent | | | |
|---|---|---|---|---|---|
| Host | Ar | $F^-$ | $Cl^-$ | $AcO^-$ | $H_2PO_4^-$ |
| **5a** | $C_6H_5$– | -242.11 | -112.51 | -125.67 | -119.77 |
| **5b** | *p*-F–$C_6H_4$– | -249.53 | -118.86 | -132.34 | -126.41 |
| **5c** | *p*-$NO_2$–$C_6H_4$– | -274.69 | -138.44 | -155.99 | -136.37 |

The heteroditopic binding properties of receptor **5b** with both $Ag^+$ and $F^-$ were also subjected to a DFT computational study. The interaction energies (Δ*IE* in DCM) for $Ag^+$⊂**5b**, **5b**⊃$F^-$, and $Ag^+$⊂[**5b**⊃$F^-$] are –169.28, –249.53, and 417.73 kJ mol$^{-1}$, respectively. The geometry-optimized structures for **5b**, **5b**⊃$F^-$and $Ag^+$⊂[**5b**⊃$F^-$]are shown in Fig. 6, and selected distances (in Å) are shown in Table 2.

**Table 2.** Selected distances (in Å) for receptor **5b** and its complexes with $F^-$, in the absence of and in the presence of $Ag^+$ (in DCM).

| | Average distances (Å) | | | |
|---|---|---|---|---|
| | pyridine (N–N') | thiourea (NH–N'H') | thiourea (NH–N'H')–$F^-$ | pyridine (N–N')–$Ag^+$ |
| Free **5b** | 6.598 | 9.095 | – | – |
| **5b**⊃$F^-$ | 9.228 | 3.073 | 1.751 | - |
| $Ag^+$⊂**5b** | 4.377 | 4.545 | – | 2.192 |
| $Ag^+$⊂[**5b**⊃$F^-$] | 4.010 | 3.049 | 1.732 | 2.332 |

## Conclusion

In summary, three new heteroditopic receptors **5a–c** based on a thiacalix[4]arene scaffold in the 1,3-*alternate* conformation have been synthesized and a limited $^1$H-NMR and Uv-vis anion complexation study was conducted. DFT computational determinations indicated that **5c** which has the strong electron–withdrawing $NO_2$ groups at the *p*-positions of the phenylthioureido moieties had the most effective recognition ability towards the selected anions. The binding of $Ag^+$ at the 2-pyridyl moieties and the binding of the anions at the two thiourea NH groups of the *p*-substituted phenylthioureido moieties, respectively, was also investigated. The appearance of a positive allosteric effect with receptor **5b** was also found using $^1$H-NMR titration experiments.

## Experimental Section

### General

All melting points were determined with Yanagimoto MP-S1. $^1$H–NMR spectra were determined at 300 MHz with a Nippon Denshi JEOL FT-300 NMR spectrometer with $SiMe_4$ as an internal reference; *J*-values are given in Hz. UV spectra were measured by a Shimadzu 240 spectrophotometer. Mass spectra were obtained on a Nippon Denshi JMS-01SG-2 mass spectrometer at an ionization energy of 70 eV using a direct inlet system through GLC. Elemental analyses were performed by Yanaco MT-5.

### Materials

Unless otherwise stated, all reagents used were purchased from commercial sources and used without further purification. 5,11,17,23-Tetra-*tert*-butyl-2,8,14,20-tetrathiacalix[4]arene-25,26,27,28-tetraol **1**[16] and *distal*-5,11,17,23-tetra-*tert*-butyl-25,27-bis(carbamoylmethoxy)-26,28-dihydroxy-2,8,14,20-tetrathiacalix[4]arene **2**[17] were prepared following the reported procedures.

### Synthesis of *distal*-5,11,17,23-tetra-*tert*-butyl-25,27-bis-(carbamoylmethoxy)-26,28-dihydroxy-2,8,14,20-tetrathia-calix[4]arene 2

A mixture of **1** (1.0 g, 1.4 mmol) and $Na_2CO_3$ (0.22 g, 1.5 mmol) in dry acetone (20 mL) was heated under reflux for 1 h under argon. Then 2-bromoacetamide (418 mg, 3.04 mmol) was added and the mixture was heated under reflux for an additional 48 h under argon. After cooling the reaction mixture to room temperature, the solvent was

evaporated under reduced pressure. The residue was made alkaline with 30% NaOH (20 mL) and extracted with $CH_2Cl_2$ (30 mL × 3). The combined extracts were washed with water (30 mL × 3) and brine (30 mL × 3). After washing, the organic layer was dried over magnesium sulfate and condensed under reduced pressure to give a crude product. Crystallization from $CHCl_3$–MeOH (3:1, v/v) gave compound **2** (738 mg, 64 %) as colourless prisms. M.p. 148–151 °C. IR (KBr)/$cm^{-1}$ 3467 (NH), 3334 (OH), 3187 (NH) and 1694 (CO). $^1$H–NMR (300 MHz, $CDCl_3$): $\delta$ = 1.05 (s, 18H, *t*Bu), 1.24 (s, 18H, *t*Bu), 4.75 (s, 4H, O$CH_2$CO), 6.19 (br, 2H, N*H*), 7.05 (br, 2H, N*H*), 7.43 (s, 4H, Ar*H*), 7.67 (s, 4H, Ar*H*) and 8.40 (s, 2H, O*H*) ppm. $^{13}$C–NMR (400 MHz, $CDCl_3$): $\delta$ = 30.9, 34.2, 68.8, 120.0, 120.7, 122.8, 123.3, 144.2, 164.8, 166.1 and 170.0 ppm. FABMS: *m/z*: 835.29 ($M^+$). Anal. calcd for $C_{44}H_{54}N_2O_6S_4$ (835.17): C 63.28, H 6.52, N 3.35; found: C 63.02, H 6.49, N 3.33.

**Synthesis of compound 3**

To a solution of **2** (1.0 g, 1.2 mmol) and $Cs_2CO_3$ (3.9 g, 12 mmol) in dry acetone (20 mL) was added 2-(chloromethyl)pyridine (2.0 g, 12 mmol) and the reaction mixture was heated under reflux for 48 h under argon. After cooling the reaction mixture to room temperature, the solvent was evaporated under reduced pressure. The residue was made alkaline with 30% NaOH (20 mL) and extracted with $CHCl_3$ (30 mL × 3). The combined extracts were washed with water (30 mL × 3) and brine (30 mL × 3). After washing, the organic layer was dried over magnesium sulfate and condensed under reduced pressure to give a crude product. The residue was purified by column chromatography using $CHCl_3$ as eluent to provide a pale-yellow powder. Crystallization from $CHCl_3$–hexane (3:1, v/v) gave compound **3** (634 mg, 52 %) as pale-yellow prisms. M.p. 195–197 °C. $^1$H–NMR (300 MHz, $CDCl_3$): $\delta$ = 0.83 (18H, s, *t*Bu), 1.28 (18H, s, *t*Bu), 4.48 (4H, s, O$CH_2$), 5.10 (2H, br, N*H*), 5.20 (4H, s, O$CH_2$), 5.51 (2H, br, N*H*), 6.57 (2H, d, *J* = 8.5 Hz, Pyridine–$H_3$), 7.09 (4H, s, Ar*H*), 7.00–7.42. (2H, m, Pyridine–$H_{4,5}$), 7.40 (4H, s, Ar*H*) and 8.51 (2H, d, *J* = 7.7 Hz, Pyridine–$H_6$) ppm. $^{13}$C NMR (400 MHz, $CDCl_3$): $\delta$ = 31.5, 31.9, 34.2, 34.3, 66.1, 70.7, 121.8, 122.0, 126.4, 126.8, 127.5, 127.8, 128.1, 135.9, 146.9, 147.0, 147.4 153.7, 155.3, 156.1 and 169.8 ppm. FABMS: *m/z*: 1017.40 ($M^+$). Anal. calcd for $C_{56}H_{64}N_4O_6S_4$ (1017.39): C 66.11, H 6.34, N 5.51; found: C 66.23, H 6.29, N 5.55.

**Synthesis of compound 4**

A solution of $BH_3$/THF (50 mL, large excess) was added to **3** (600 mg, 0.590 mmol) and the reaction mixture was heated under reflux for 20 h under argon. After cooling the reaction mixture to room temperature, it was quenched by the slow addition of aqueous 1.0 M HCl (30 mL). The mixture was again heated at reflux for 1 h under argon. After cooling the reaction mixture to room temperature, the solvent was evaporated under reduced pressure. The residue was made alkaline with 30% NaOH (20 mL) and extracted with $CHCl_3$ (30 mL × 3). The combined extracts were washed with water (30 mL × 3) and brine (30 mL × 3). After washing, the organic layer was dried over magnesium sulfate and condensed under reduced pressure to give a crude product. The residue was purified by column chromatography using $CHCl_3$–MeOH (10:1) as eluent to provide a colourless powder. Crystallization from $CHCl_3$–hexane (7:3, v/v) gave compound **4** (479 mg, 82 %) as colourless prisms. M.p. 180–182 °C. $^1$H–NMR (300 MHz, $CDCl_3$): $\delta$ = 0.82 (18H, s, *t*Bu), 1.31(18H, s, *t*Bu), 2.20 (4H, br, N$H_2$), 2.52 (4H, t, *J* = 9.0 Hz, $OCH_2CH_2NH_2$), 4.02 (t, *J* = 9.0Hz, 4H, $OCH_2CH_2NH_2$), 5.12 (s, 4H, Pyridine–$CH_2$), 6.50 (2H, d, *J* = 8.5 Hz, Pyridine–$H_3$), 7.05 (s, 4H, Ar–*H*), 7.13 (2H, br, Pyridine–$H_4$), 7.42 (s, 4H, Ar–*H*), 7.49–7.60. (2H, m, Pyridine–$H_5$) and 8.49 (2H, d, *J* = 7.7 Hz, Pyridine–$H_6$) ppm. $^{13}$C–NMR (400 MHz, $CDCl_3$): $\delta$ = 30.0, 33.8, 33.9, 68.9, 70.6, 120.0, 128.1, 128.5, 128.8, 129.4, 129.9, 136.0, 149.8, 150.5, 150.8, 154.0, 156.4 and 158.0 ppm. FABMS: *m/z*: 989.40 ($M^+$). Anal. calcd for $C_{56}H_{68}N_4O_4S_4$ (989.43): C 67.89, H 6.93, N 5.66; found: C 67.45, H 6.50, N 5.45.

**Synthesis of compound 5a**

To compound **4** (100 mg, 0.101 mmol) in dry $CH_2Cl_2$ (15 mL) was added phenyl isothiocyanate (82 mg, 0.61 mmol) and the mixture was stirred at room temperature for 12 h under argon. The solvent was then evaporated under reduced pressure. The residue was purified by column chromatography using $CHCl_3$–MeOH–aqueous 28% $NH_3$ solution (95:4:1, v/v) as eluent to provide a colourless powder. Crystallization from $CHCl_3$–Hexane (3:1, v/v) gave **5a** (94 mg, 74 %) as colourless prisms. M.p. 223–224 °C. $^1$H–NMR (300 MHz, $CDCl_3$–DMSO-$d_6$, 10:1, v/v): $\delta$ = 0.87 (18H, s, *t*Bu), 1.29 (18H, s, *t*Bu), 3.52 (4H, br, $OCH_2CH_2$NH), 4.10 (4H, br, $OCH_2CH_2$NH), 5.12 (4H, s, Pyridine–$CH_2$), 6.70 (2H, d, *J* = 7.8 Hz, Pyridine–$H_3$), 7.03 (4H, s, Ar–*H*), 7.10–7.70. (m, 16H, Phenyl–*H*, $CH_2$N*H* and Pyridine–$H_{4,5}$), 7.46 (4H, s, Ar–*H*), 7.72 (2H, s, Phenyl–N*H*) and 8.60 (2H, s, Pyridine–$H_6$) ppm. $^{13}$C–NMR (400 MHz, $CDCl_3$–DMSO-$d_6$, 10:1, v/v): $\delta$ = 30.7, 34.0, 45.9, 64.8, 68.8, 122.3, 124.0, 126.2, 129.2, 130.1, 131.2, 132.4, 134.5, 136.0, 146.0, 146.3, 155.3, 156.0, 169.4 and 182.0 ppm. FABMS: *m/z*: 1259.46 ($M^+$). Anal. calcd for $C_{70}H_{78}N_6O_4S_6$ (1259.80): C 66.74, H 6.24 N 6.67; found: C 66.69, H 6.32, N 6.76.

**Synthesis of compound 5b**

To compound **4** (100 mg, 0.101 mmol) in dry $CH_2Cl_2$ (15 mL) was added 4-fluorophenyl isothiocyanate (93 mg, 0.61 mmol) and the mixture was stirred at room temperature for 12 h under argon. The solvent was then evaporated under reduced pressure. The residue was purified by column chromatography using $CHCl_3$–MeOH–28% aqueous $NH_3$ solution (95:4:1) as eluent to provide a colourless powder. Recrystallization from $CHCl_3$–Hexane (3:1, v/v) gave receptor **5b** (102 mg, 78 %) as colourless prisms. M.p. 209–210 °C. $^1$H–NMR (300 MHz, $CDCl_3$–DMSO-$d_6$, 10:1, v/v): $\delta$ = 0.82 (18H, s, *t*Bu), 1.12 (18H, s, *t*Bu), 3.49 (4H, br, $OCH_2CH_2$NH), 4.10 (4H, br, $OCH_2CH_2$NH), 5.13 (4H, s, Pyridine–$CH_2$), 6.68 (2H, d, *J* = 7.8 Hz, Pyridine–$H_3$), 7.04 (4H, s, Ar–*H*), 6.88–7.80. (m, 14H, *p*–F–$C_6H_4$, $CH_2$N*H* and Pyridine–$H_{4,5}$), 7.40 (4H, s, Ar–*H*), 8.06 (2H, br, *p*–F–$C_6H_4$–N*H*) and 8.50 (2H, s, Pyridine–$H_6$) ppm. $^{13}$C–NMR (400 MHz, $CDCl_3$– DMSO-$d_6$, 10:1, v/v): $\delta$ = 31.0, 34.0, 44.8, 66.0, 69.9, 121.8, 122.6, 124.0, 124.3, 126.1, 126.5, 128.3, 131.9, 132.4, 133.0, 133.8, 135.2, 135.9, 146.8, 148.2, 155.1, 155.6, 156.2, 156.4, 160.0, 160.7 and 181.8 ppm. FABMS: *m/z*: 1295.5188 ($M^+$). $C_{70}H_{76}F_2N_6O_4S_6$

(1295.5386): calcd C 64.88, H 6.49, N 5.91; found: C 64.76, H 6.33, N 5.76.

### Synthesis of compound 5c

To compound **4** (100 mg, 0.101 mmol) in dry $CH_2Cl_2$ (15 mL) was added 4-nitrophenyl isothiocyanate (109 mg, 0.606 mmol) and the mixture was stirred for at room temperature for 12 h under argon. After the reaction, the solvent was evaporated under reduced pressure. The residue was purified by column chromatography using $CHCl_3$–MeOH– aqueous 28% $NH_3$ solution (95:4:1, v/v) as eluent to provide a colourless powder. Crystallization from $CHCl_3$–$CH_3CN$ (3:2, v/v) gave receptor **5c** (98 mg, 72 %) as pale–yellow prisms. M.p. 206–207 °C. $^1$H–NMR (300 MHz, $CDCl_3$– DMSO-$d_6$, 10:1, v/v): $\delta$ = 0.82 (18H, s, *t*Bu), 1.31 (18H, s, *t*Bu), 3.50 (4H, br, $OCH_2CH_2NH$), 4.10 (4H, br, $OCH_2CH_2NH$), 5.19 (4H, s, Pyridine–$CH_2$), 6.69 (2H, d, $J$ = 7.8 Hz, Pyridine–$H_3$), 7.10 (4H, s, Ar–*H*), 7.20–7.68. (4H, m, Pyridine–$H_{4,5}$), 7.53 (4H, s, Ar–*H*), 7.80 (4H, d, $J$ = 9.0 Hz, *p*–$NO_2$–$C_6H_4$), 8.15 (4H, d, $J$ = 9.0 Hz, *p*–$NO_2$–$C_6H_4$), 8.50 (2H, s, Pyridine–$H_6$), 8.70 (2H, br, $CH_2NH$ ), and 9.72 (2H, br, *p*–$NO_2$–$C_6H_4$–N*H*) ppm. $^{13}$C–NMR (400 MHz, $CDCl_3$–DMSO-$d_6$, 10:1, v/v): $\delta$ = 30.2, 34.0, 44.1, 66.0, 71.3, 120.1, 122.0, 125.8, 127.0, 128.2, 129.6, 131.2, 132.4, 134.0, 134.9, 136.0, 138.0, 148.1, 151.0, 156.1, 157.7, 158.4, 164.0 and 183.9 ppm. FABMS: *m/z*: 1349.4189 ($M^+$). $C_{70}H_{76}N_8O_8S_6$ (1349.5154): calcd C 62.29, H 5.68, N 8.30.

### Determination of the Association Constants

The association constants were determined using $^1$H-NMR spectroscopic titration experiments at a constant concentration of host receptor ($4.0 \times 10^{-3}$ M) and varying the guest concentration (0–$8.0 \times 10^{-3}$ M). The $^1$H-NMR chemical shifts of the thiourea protons (NH) signal were used as a probe. The association constants ($K_a$) for the complexes of receptors **5a** and **5b** with *n*-$Bu_4NF$ were calculated using the *Bindfit* global fit analysis method[20] for the chemical shift changes of the thiourea NH protons. The solvent used was a 10:1:1, v/v mixture of $CDCl_3$–DMSO-$d_6$–$CD_3CN$). For the allosteric behavour experiments, the same solvent system was used for the titration of **5b** (and its 1:1 $F^-$ complex) in the absence of, and also in the presence of $AgSO_3CF_3$.

### UV–vis Experiments

Qualitative titration experiments with solutions of **5a-c** in $CH_2Cl_2$ were investigated by the addition of aliquots of the anions as their TBA salts (0–50 μM) in $CH_2Cl_2$–DMSO (10:1, v/v), the respective. The Job plot[22] experiments were conducted in the same solvent system.

### Single-crystal X-ray crystallographic analysis of 5a

Crystal *data for* **5a**: $C_{70}H_{78}N_6O_4S_6 \cdot C_{57}H_{67}N_4O_4S_4^+ \cdot Cl^- \cdot CHCl_3$, $M_r$ =2415.05. Orthorhombic, *Pbca*; $a$ =26.9078 (10), $b$ =27.1717 (11), $c$ = 34.4369 (13) Å; $V$ = 25177.9 (17) Å$^3$; $Z$ = 8; $D_x$ = 1.274 Mg m$^{-3}$; $F$(000) =10208; $T$ = 150 K; $\mu$ = 0.40 mm$^{-1}$; λ = 0.7749 Å, crystal size 0.15 × 0.15 × 0.03 mm$^3$. Crystals were yellow blocks. Diffraction data were measured at ALS Station 11.3.1 using synchrotron radiation on a Bruker D8 with PHOTON 100 detector diffractometer equipped with a silicon 111 monchromator using thin-slice ω-scans.[25] 218318 measured reflections, 23240 independent reflections ($R_{int}$ = 0.055) to $\theta_{max}$ = 27.9°; 17514 reflections with $I > 2\sigma(I)$. The structure was determined by iterative, dual-space methods using the *SHELXT* program and refined by the full-matrix least-squares method, on $F^2$, in *SHELXL-2013/14*.[26–27] The non-hydrogen atoms were refined with anisotropic thermal parameters. Hydrogen atoms on C were included in idealized positions and their $U_{iso}$ values were set to ride on the $U_{eq}$ values of the parent atoms. H atoms on N were freely refined. At the conclusion of the refinement, $wR_2$ = 0.156 (all data) and $R_1$ = 0.051 (observed data), 1520 parameters, $\Delta\rangle_{max}$ = 0.61 eÅ$^{-3}$; $\Delta\rangle_{min}$ = –0.88 eÅ$^{-3}$; 134 restraints. The choroform molecule was modeled as disordered over two, closely-spaced sites with major site occupancy of 68.1(6) %. The crystallographic data (excluding structure factors) for the structure in this paper have been deposited with the Cambridge Crystallographic Data Centre as supplementary publication number CCDC 2075593 for **5a**.


### Acknowledgements

This work was performed under the Cooperative Research Program of "Network Joint Research Center for Materials and Devices (Institute for Materials Chemistry and Engineering, Kyushu University)". We would like to thank the OTEC at Saga University for financial support. CR thanks the EPSRC for a travel grant (EP/R023816/1). The Advanced Light Source is supported by the Director, Office of Science, Office of Basic Energy Sciences, of the U.S. Department of Energy under Contract No. DE-AC02-05CH11231. AA thanks Researchers Supporting Project Number (RSP-2021/304), King Saud University, Riyadh, Saudi Arabia. Compute Canada is thanked for providing the ongoing computing resources to PEG and SR.


### Notes and references


[a] Department of Applied Chemistry, Faculty of Science and Engineering, Saga University, Honjo-machi 1, Saga 840-8502 Japan. E-mail: yamatot@cc.saga-u.ac.jp

[b] School of Chemical Engineering, Shandong University of Technology, Zibo 255049, P. R. China.

[c] Department of Chemistry, Memorial University of Newfoundland St. John's, Newfoundland and Labrador A1B 3X7, Canada.

[d] Department of Physics and Astronomy, College of Science, King Saud University, Riyadh 11451, Saudi Arabia.

[e] Chemistry Department, Loughborough University, Loughborough LE11 3TU, UK.

[f] ALS, Berkeley Lab, 1 Cyclotron Road, Bereleley, CA 94720, USA.

[g] Department of Chemistry, The University of Hull, HU6 7RX, UK.


† Electronic Supplementary Information (ESI) available: Details of the $^1$H/$^{13}$C–NMR spectra, Crystallographic data, $^1$H–NMR

spectroscopic and UV-vis titration experimental data, and Job plot, See DOI:10.1039/b000000x/


1 (*a*) C. D. Gutsche, *Calixarenes, An Introduction,* Royal Society of Chemistry*:* Cambridge, UK, 2008; (*b*) Neri, P., J. L. Sessler, M.-X. Wang, Eds., *Calixarenes and Beyond*; Springer International Publishing AG, Switzerland, 2016. (*c*) Z. Asfari, V. Böhmer, J. Harrowfield, J. Vicens, (Eds.) *Calixarenes 2001*; Kluwer Acad. Publ.: Dordrecht, 2001.

2 (*a*) N. Iki pp 335-362, *In Calixarenes and Beyond*; Neri, P., J. L. Sessler, M.-X. Wang, Eds., Springer International Publishing AG, Switzerland, 2016; (*b*) H. Kumagi, M. Hasegawa, S. Miyanari, Y. Sugawa, Y. Sato, T. Hori, S. Ueda, H. Kamiyama and S. Miyano, *Tetrahedron Lett.,* 1997, **38**, 3971–3972.

3 (*a*) P. Lhoták, *Eur. J. Org. Chem.*, 2004, 1675–1692; (*b*) N. Morohashi, F. Narumi, N. Iki, T. Hattori and S. Miyano, *Chem. Rev.,* 2006, **106**, 5291–5316; (*c*) M. H. Noamane, S. Ferlay, R. Abidi, N. Kyritsakas and M. W. Hosseini, *Eur. J. Inorg. Chem.*, 2017, **27**, 3327–3336; (*d*) A. A. Vavilova and I. I. Stoikov, *Beilstein J. Org. Chem.*, 2017, **13**, 1940–1949; (*e*) O. A. Mostovaya, P. L. Padnya, A. A. Vavilova, D. N. Shurpik, B. I. Khairutdinov, T. A. Mukhametzyanov, A. A. Khannanov, M. P. Kutyreva and I. I. Stoikov, *New J. Chem.*, 2018, **42**, 177–183; (*f*) A. A. Vavilova, V. V. Gorbachuk, D. N. Shurpik, B. I. Khairutdinov, (*d*) A. A. Vavilova, V. V. Gorbachuk, D. N. Shurpik, A. V. Gerasimov, L. S. Yakimova, P. L. Padnya and I. I. Stoikov, *J. Mol. Liq.*, 2019, **281**, 243–251; (*g*) T. A. Mukhametzyanov and I. I. Stoikov, *Nanomaterials*, 2020, ***10***, 777; (*h*) P. Padnya, K. Shibaeva, M. Arsenyev, S. Baryshnikova, O. Terenteva, I. Shiabiev, A. Khannanov, A. Boldyrev, A. Gerasimov, D. Grishaev, Y. Shtyrlin and I. Stoikov, *Molecules,* 2021, ***26***, 2334; (*i*) O. A. Mostovaya, P. L. Padnya, D. N. Shurpik, I. E. Shiabiev and I. I. Stoikov, *J. Mol. Liq.*, 2021, **327**, 114806.

4 S. Rahman, H. Tomiyasu, H. Kawazoe, J.–L. Zhao, H. Cong, X.–L. Ni, X. Zeng, M. R. J. Elsegood, T. G. Warwick, S. J. Teat, C. Redshaw, P. E. Georghiou and T. Yamato, *New J. Chem.,* 2016, **40**, 9245–9251.

5 (*a*) P. D. Beer and P. A. Gale, *Angew. Chem. Int. Ed.,* **2001**, 40, 486–516; (*b*) T. Nabeshima, T. Saiki and S. Kumitomo, *Org. Lett*., 2002, **4**, 3207–3209; (*c*) T. Nabeshima, Y. Yoshihira, T. Saiki, S. Akine and E. Horn, *J. Am. Chem. Soc.,* 2003, **125**, 28–29; (*d*) A. Y. Zhukov, T. A. Fink, I. I. Stoikov and I. S. Antipin, *Russ. Chem. Bull., Int. Ed.,* 2009, **58**, 1007–1014; (*e*) K. Mohr, J. Schmitz, R. Schrage, C. Trnkle and U. Holzgrabe, *Angew. Chem. Int. Ed*., 2013, **52**, 508–516; (*f*) R. Nussinov and C.–J. Tsai, *Cell,* 2013, **153**, 293–305.

6 (*a*) C. Perez-Casas and T. Yamato, *J. Incl. Phenom. Macrocyclic Chem.,* 2005, **53**, 1–8; (*b*) T. Yamato, C. Perez-Casas, H. Yamamoto, M. R. J. Elsegood, S. H. Dale and C. Redshaw, *J. Incl. Phenom. Macrocyclic Chem.,* 2006, **54**, 261–269; (*c*) C. Perez-Casas, S. Rahman, N. Begum, Z. Xi and T. Yamato, *J. Incl. Phenom. Macrocyclic Chem.*, 2008, **60**, 173–185; (*d*) X.-L. Ni, X. Zeng, C. Redshaw and T. Yamato, *Tetrahedron*, 2011, **67**, 3248–3253; (*e*) X.–L. Ni, J. Tahara, S. Rahman, X. Zeng, D. L. Hughes, C. Redshaw and T. Yamato, *Chem. Asian. J.*, 2012, **7**, 519–527; (*f*) X.–L. Ni, H. Cong, A. Yoshizawa, S. Rahman, H. Tomiyasu, U. Rayhan, X. Zeng and T. Yamato, *J. Mol. Struct.*, 2013, **1046**, 110–115.

7 (*a*) J.-L. Zhao, H. Tomiyasu, X.–L. Ni, X. Zeng, M. R. J. Elsegood, C. Redshaw, S. Rahman, P. E. Georghiou and T. Yamato, *New J. Chem.,* 2014, **38**, 6041– 6049; (*b*) J.-L. Zhao, H. Tomiyasu, X.–L. Ni, X. Zeng, M. R. J. Elsegood, C. Redshaw, S. Rahman, P. E. Georghiou, S. J. Teat and T. Yamato, *Org. Biomol. Chem.,* 2015, **13**, 3476–3483; (*c*) J.–L. Zhao, H. Tomiyasu, C. Wu, H. Cong, X. Zeng, S. Rahman, P. E. Georghiou, D. L. Hughes, C. Redshaw and T. Yamato, *Tetrahedron*, 2015, **71**, 8521–8527; (*d*) J.–L. Zhao, C. Wu, H. Tomiyasu, X. Zeng, M. R. J. Elsegood, C. Redshaw and T. Yamato, *Chemistry Asian J.,* 2016, **11**, 1606–1612; (*e*) J.–L. Zhao, C. Wu, X. Zeng, S. Rahman, P. E. Georghiou, M. R. J. Elsegood, T. G. Warwick, C. Redshaw, S. J. Teat and T. Yamato, *ChemistrySelect*, 2016, **1**, 1541–1547; (*f*) J.–L. Zhao, X.-K. Jiang, C. Wu, C.-Z. Wang, X. Zeng, C. Redshaw and T. Yamato, *ChemPhyChem*, 2016, **17**, 3217–3222.

8 (*a*) H. Tomiyasu, J.–L. Zhao, X.–L. Ni, X. Zeng, M. R. J. Elsegood, B. Jones, C. Redshaw, S. J. Teat and T. Yamato, *RSC Adv.*, 2015, **5**, 14747–14755; (*b*) M.–Q. Ran, J.–Y. Yuan, Y.–H. Zhao, L. Mu, X. Zeng, C. Redshaw, L. Jiang and T. Yamato, *Supramolecular Chemistry*, 2016, **28**, 418–426.

9 (*a*) J. L. Sessler, P. A. Gale and W. S. Cho, Anion Receptor Chemistry; Royal Society of Chemistry: Cambridge, U.K., 2006; (*b*) P. D. Beer, P. A. Gale, *Angew. Chem., Int. Ed*., 2001, **40**, 486–516.

10 (*a*) J.–Y Kwon, Y.–J Jang, S.–K Kim, K.–H Lee, J.–S Kim and J. Yoon, *J. Org. Chem.,* 2004, ***69***, 5155–5157; (*b*) D. Amilan Jose, D. K. Kumar, B. Ganguly and A. Das, *Org. Lett.*, 2004, **6**, 3445–3448; (*c*) J.–Y. Lee, E.–J Cho, S. Mukamel and K.–C. Nam, *J. Org. Chem.*, 2004, **69**, 943–950; (*d*) D. Esteban-Gomez, L. Fabbrizzi and M. Licchelli, *J. Org. Chem.,* 2005, ***70***, 5717–5720; (*e*) V. Thiagarajan, P. Ramamurthy, D. Thirumalai and V. T. Ramakrishnan, *Org. Lett.*, 2005, **7**, 657–660; (*f*) H. Lu, W. Xu, D. Zhang, C. Chen and D. Zhu, *Org. Lett.*, 2005, **7**, 4629–4632; (*g*) F. M. Pfeffer, T. Gunnlaugsson, P. Jensen and P. E. Kruger, *Org. Lett.*, 2005, **7**, 5357–5360; (*h*) L. Fang, W.–H. Chan, Y.–B. He, D. W.–J. Kwong and A. W.–M. Lee, *J. Org. Chem.,* 2005, **70**, 7640–7646; (*i*) T. Gunnlaugsson, P. E. Kruger, P. Jensen, J. Tierney, H. D. Paduka Ali and G. M. Hussey, *J. Org. Chem.*, 2005, **70**, 10875–10878; (*j*) A. Dahan, T. Ashkenazi, V. Kuznetsov, S. Makievski, E. Drug, L. Fadeev, M. Bramson, S. Schokoroy, E. Rozenshine–Kemelmakher and M. Gozin, *J. Org. Chem.,* 2007, **72**, 2289–2296; (*k*) S. Saha, A. Ghosh , P. Mahato , S. Mishra , S. K. Mishra, E. Suresh , S. Das and A. Das, *Org. Lett.*, 2010, **12**, 3406–3409.

11 (a) J. F. Zhang, Y. Zhou, J. Yoon and J. S. Kim, *Chem. Soc. Rev*., 2011, **40**, 3416–3429; (b) C. Lodeiro, J. L. Capelo, J. C. Mejuto, E. Oliveira, H. M. Santos, B. Pedras and C. Nuñez, *Chem. Soc. Rev*., 2010, **39**, 2948–2976; (c) L. E. Santos-Figueroa, M. E. Moragues, E. Climent, A. Agostini, R. Martínez-Máñez and F. Sancenón, *Chem. Soc. Rev*., 2013, **42**, 3489–3613.

12 (*a*) R. M. F. Batista, E. Oliveira, S. P. G. Costa, C. Lodeiro and M. M. M. Raposo, *Org. Lett.* 2007, **9**, 3201–3204; (*b*) F. Zapata, A. Caballero, A. Espinosa, A. Tárraga, and P. Molina, *Org. Lett.*, 2008, **10**, 41–44; (*c*) R. D. Rasberry, M. D. Smith and K. D. Shimizu, *Org. Lett.* 2008, **10**, 2889–2892; (*d*) C. Pérez-Casas and A. K. Yatsimirsky, *J. Org. Chem.*, 2008, **73**, 2275–2284; (*e*) J. P. Clare, A. Statnikov, V. Lynch, A. L. Sargent and J. W. Sibert, *J. Org. Chem.*, 2009, **74**, 6637–6646; (*f*) Q.–S Lu, L. Dong, J. Zhang, J. Li, L. Jiang, Y. Huang, S. Qin, C.–W. Hu and X.–Q. Yu, *Org. Lett.*, 2009, **11**, 669–672; (*g*) S. Goswami, D. Sen and N. K. Das, *Org. Lett.*, 2010, **12**, 856–859; (*h*) A. Aldrey, C. Núñez, V. García, R. Bastida, C. Lodeiro, A. Macías, *Tetrahedron*, 2010, **66**, 9223–9230; (*i*) P. Dydio, T. Zieliński and J. Jurczak, *Org. Lett.*, 2010, **12**, 1076–1078; (*j*) V. K. Bhardwaj, S. Sharma, N. Singh, M. S. Hundal and G. Hundal, *Supramol. Chem.*, 2011, **23**, 790–800; (*k*) G.–W. Lee, N.–K. Kim and K.–S. Jeong, *Org. Lett.*, 2011, **13**, 3024–3027; (*l*) H. M. Chawla, S. N. Sahu, R. Shrivastava, S. Kumar, *Tetrahedron Lett*., 2012, **53**, 2244–2247; (*m*) S. Goswami, A. Manna, S. Paul, K. Aich, A. K. Das and S. Chakraborty, *Tetrahedron Lett.*, 2013, **54**, 1785–1789; (*n*) K. Pandurangan, J. A. Kitchen and T. Gunnlaugsson, *Tetrahedron Lett.*, 2013, **54**, 2770–2775; (*o*) S. Areti, J. K. Khedkar, R. Chilukula and C. P. Rao, *Tetrahedron Lett*., 2013, **54**, 5629–5634; (*p*) C. Jin, M. Zhang, C. Deng, Y. Guan, J. Gong, D. Zhu, Y. Pan, J. Jiang and L. Wang, *Tetrahedron Lett.*, 2013, **54**, 796–801.

13 (*a*) K. Lang, P. Cuřínová, M. Dudič, P. Proščová, I. Stibor, V. Št'astný and P. Lhoták, *Tetrahedron Lett.*, 2005, **46**, 4469–4472; (*b*) P. Lhoták, J. Svoboda and I. Stibor, *Tetrahedron Lett.*, 2006, **62**, 1253–1257; (*c*) J. Kroupa, I. Stibor, M. Pojarová, M. Tkadlecová and P. Lhoták, *Tetrahedron*, 2008, **64**, 10075–10079; (*d*) O. Kundrat, H. Dvorakova, I. Cisarova, M. Pojarova and P. Lhoták, *Org. Lett.*, 2009, **11**, 4188–4191; (*e*) O. Kundrat, I. Cisarova, S. Böhm, M. Pojarova and P. Lhoták, *J. Org. Chem.*, 2009, **74**, 4592–4596; (*f*) O. Kundrat, H. Dvorakova, V. Eigner and P. Lhoták, *J. Org. Chem.*, 2010, **75**, 407–411; (*g*) O. Kundrat, J. Kroupa, S. Böhm, J. Budka, V. Eigner and P. Lhoták, *J. Org. Chem.*, 2010, **75**, 8372–8375; (*h*) O. Kundrát, V. Eigner, P. Cuřínová, J. Kroupa and P. Lhoták, *Tetrahedron*, 2011, **67**, 8367–8372; (*i*) O. Kundrat, V. Eigner, H. Dvorakova, and P. Lhoták, *Org. Lett.*, 2011, **13**, 4032–4035; (*j*) P. Slavik, M. Dudic, K. Flidrova, J. Sykora, I. Cisarova, M. Pojarova and P. Lhoták, *Org. Lett.*, 2012, **14**, 3628–3631; (*k*) O. Kundrat, H. Dvorakova, S. Böhm, V. Eigner and P. Lhoták, *J. Org. Chem.*, 2012, **77**, 2272–2278.

14 (*a*) V. Bhalla, M. Kumar, H. Katagiri, T. Hattori and S. Miyano, *Tetrahedron Lett*., 2005, **46**, 121–124; (*b*) V. Bhalla, J. N. Babu, M. Kumar, T. Hattori and S. Miyano, *Tetrahedron Lett.,* 2007, **48**, 1581–1585; (*c*) V. Bhalla, R. Kumar, M. Kumar and A. Dhir, *Tetrahedron*, 2007, **63**, 11153–11159; (*d*) A. Dhir, V. Bhalla and M. Kumar, *Org. Lett*., 2008, **10**, 4891–4894; (*e*) R. Kumar, V. Bhalla and M. Kumar, *Tetrahedron*, 2008, **64**, 8095–8101; (*f*) R. K. Mahajan, R. Kaur, V. Bhalla, M. Kumar, T. Hattori and S. Miyano, *Sens. Actuators B*, 2008, **130**, 290–294; (*g*) J. N. Babu, V. Bhalla, M. Kumar, R. K. Mahajan and R. K. Puri, *Tetrahedron Lett.*, 2008, **49**, 2772–2775; (*h*) M. Kumar, A. Dhir and V. Bhalla, *Org. Lett*., 2009, **11**, 2567–2570; (*i*) M. Kumar, R. Kumar and V. Bhalla, *Tetrahedron,* 2009, **65**, 4340–4344 (*j*) M. Kumar, A. Dhir and V. Bhalla; *Org. Lett.,* 2009, **11**, 2567–2570; (*k*) M. Kumar, R. Kumar and V. Bhalla, *Tetrahedron Lett*., 2010, **51**, 5559–5562; (*l*) M. Kumar, R. Kumar and V. Bhalla, *Org. Lett.*, 2011, **13**, 366–369; (*m*) M. Kumar, R. Kumar and V. Bhalla, *Org. Bio. Chem.*, 2011, **9**, 8237–8245; (*n*) M. Kumar, R. Kumar and V. Bhalla, *Org. Lett.*, 2011, **13**, 366–369; (*o*) M. Kumar, R. Kumar and V. Bhalla, *Tetrahedron Lett.*, 2013, **54**, 1524–1527.

15 S. Bartz, D. T. Schühle, J. A. Peters and J. Schatz, *Z. Naturforsch*, 2016, **71**, 113–118.

16 (*a*) N. Iki, F. Marumi, T. Fujimoto, N. Morohashi and S. Miyano, *J. Chem. Soc. Perkin Trans. 2*, **1998**, 2745; (*b*) N. Iki, N. Morohashi, F. Narumi, T. Fujimoto, T. Suzuki and S. Miyano, *Tetrahedron. Lett.*, 1999, **40**, 7337–7341.

17 S. Rahman, T. Shimizu, Z. Xi and T. Yamato, *J. Chem. Research*, **2009**, 1–4.

18 For the the Cambridge Structural Database: C. R. Groom, I. J. Bruno, M. P. Lightfoot and S. C. Ward, *Acta Crystallogr*., *Sect. B: Struct. Sci. Cryst. Eng. & Mat*., 2016, **72**, 171–179.

19 We have previously noted the interaction of tetrabutylammonium salts with $CHCl_3$: H. F. Sleem, L. N. Dawe, S. Rahman, and P. E. Georghiou, *Supramol. Chem.* 2014*,* **26***,* 579–582.

20 (*a*) P. Thordarson, *Chem. Soc. Rev*., 2011, **40**, 1305–1323; (*b*) *http://supramolecular.org*.

21 (*a*) Z. Zhang and P. R. Schreiner, *Chem. Soc. Rev.,* 2009, **38**, 1187–1198; (*b*) F. Kniep, S. H. Jungbauer, Q. Zhang, S. M. Walter, S. Schindler, I. Schnapperelle, E. Herdtweck and S. M. Huber, *Angew. Chem. Int. Ed.,* 2013, **52**, 7028–7124; (*c*) L. S. Evans, P. A. Gale, M. E. Light and R. Quesada, *Chem. Commun.,* 2006, **42**, 965–967; (*d*) C. Pérez-Casas and A. K. J. Yatsimirsky, *Org. Chem.,* 2008, **73**, 2275–2284; (*e*) M. Raposo, B. García-Acosta, T. Ábalos, P. Calero, R. Martínez-Mánez, J. V. Ros-Lis and J. Soto, *J. Org. Chem.,* 2010, **75**, 2922–2933.

22 P. Job, *Ann. Chim.*, 1928, **9**, 113–203.

23 M. J. Frisch, *et al*., *Gaussian 16*, Revision C.01 Gaussian, Inc., Wallingford CT, 2019.

24 (a) J. P. Perdew, K. Burke, M. Ernzerhof, *Phys. Rev. Lett.* 1996, **77**, 3865; (b) J. P. Perdew, K. Burke, M. Ernzerhof, *Phys. Rev. Lett.* 1997, **78**, 1396.

25 SAINT and APEX 2 (2008) software for CCD diffractometers. Bruker AXS Inc., Madison, USA.

26 G. M. Sheldrick, *Acta Crystallogr., Sect. A: Found. Crystallogr.*, 2015, **71**, 3–8.

27 G. M. Sheldrick, *Acta Crystallogr*., *Sect. C: Struct. Chem.*, 2015, **71**, 3–8.

**Allosteric binding properties of a 1,3-*alternate* thiacalix[4]arene-based receptor having phenyl-thiolurea and 2-pyridylmethyl moieties on opposite faces**

Shofiur Rahman,[a,c] Hirotsugu Tomiyasu,[a] Chuan-Zeng Wang,[a,b] Paris E. Georghiou,[c*] Abdullah Alodhayb, [d] Cameron L. Carpenter-Warren,[e] Mark R. J. Elsegood,[e] Simon J. Teat,[f] Carl Redshaw,[g] and Takehiko Yamato[a*]

Thiacalix[4]arene receptors with two thiourea moieties and two 2-pyridyl moieties exhibited a heteroditopic dinuclear receptor with $F^-$ and $Ag^+$ ions by a positive allosteric effect.

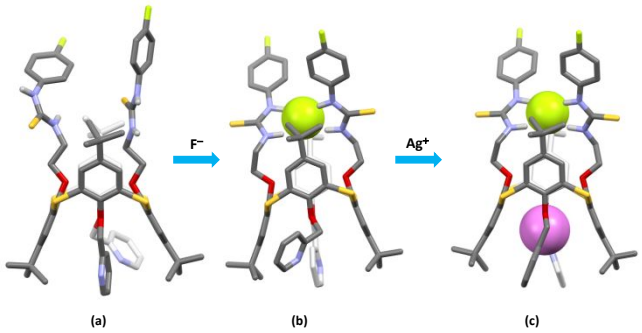

# SUPPORTING INFORMATION

Manuscript title: **Allosteric binding properties of a 1,3-*alternate* thiacalix[4]arene-based receptor having phenylthiolurea and 2-pyridylmethyl moieties on opposite faces**

Author(s): Shofiur Rahman,[a,c] Hirotsugu Tomiyasu,[a] Chuan-Zeng Wang,[a,b] Paris E. Georghiou,[c*] Abdullah Alodhayb,[d] Cameron L. Carpenter-Warren,[e] Mark R. J. Elsegood,[e] Simon J. Teat,[f] Carl Redshaw,[g] and Takehiko Yamato[a*]

[a] Department of Applied Chemistry, Faculty of Science and Engineering, Saga University, Honjo–machi 1, Saga 840–8502 Japan, E–mail: yamatot@cc.saga-u.ac.jp

[b] School of Chemical Engineering, Shandong University of Technology, Zibo 255049, P. R. China

[c] Department of Chemistry, Memorial University of Newfoundland St. John's, Newfoundland and Labrador A1B 3X7, Canada

[d] Department of Physics and Astronomy, College of Science, King Saud University, Riyadh 11451, Saudi Arabia

[e] Chemistry Department, Loughborough University, Loughborough, LE11 3TU, UK

[f] ALS, Berkeley Lab, 1 Cyclotron Road, Berkeley, CA 94720, USA

[g] Department of Chemistry, The University of Hull, Cottingham Road, Hull, Yorkshire, HU6 7RX, UK

**Table of Contents** (**S1** to **S18** are the page numbers)

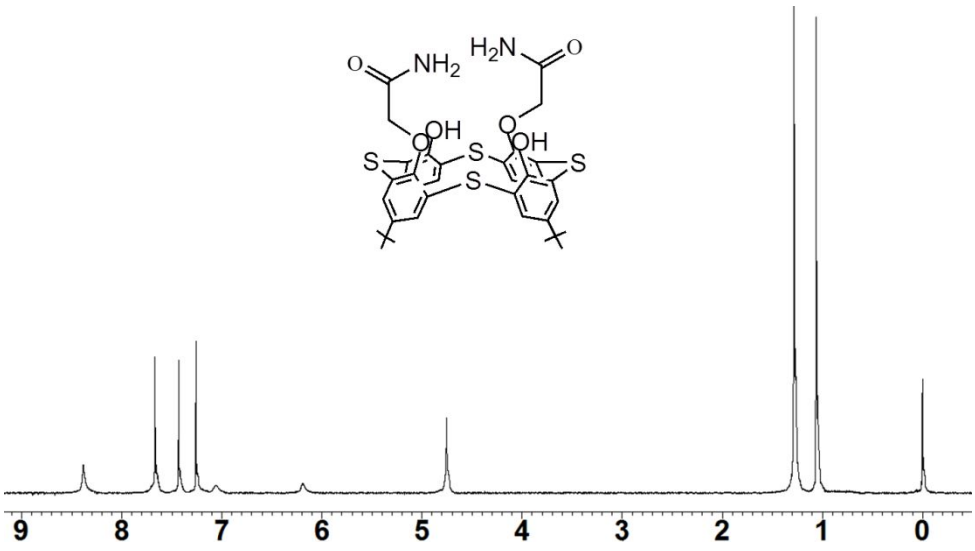


**Figure S1**. $^{1}$H–NMR spectrum of **2** (300 MHz, $CDCl_3$, 293 K).

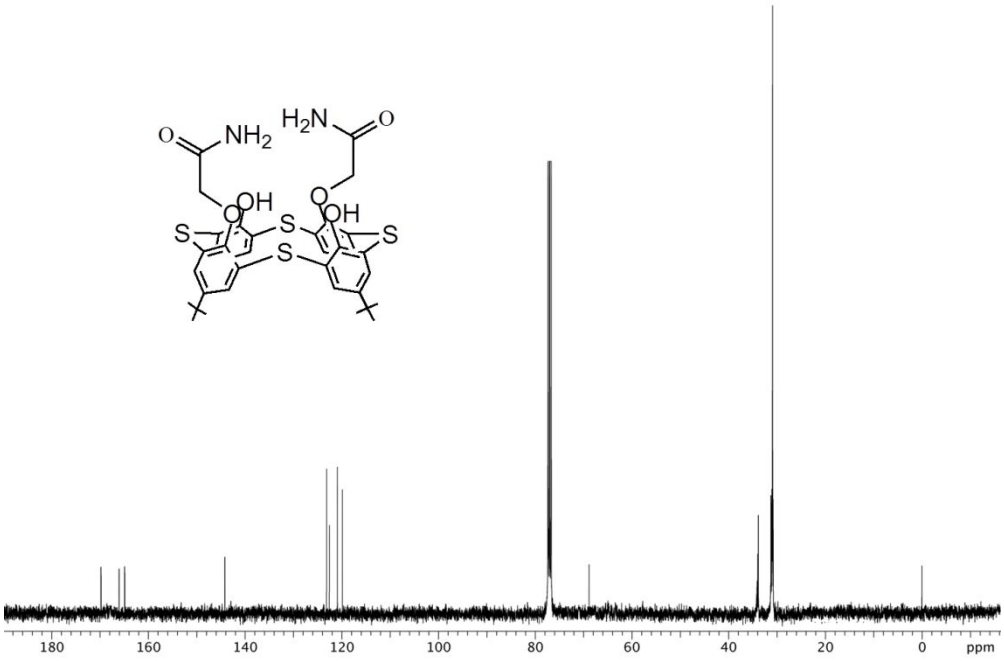


**Figure S2**. $^{13}$C–NMR spectrum of **2** (400 MHz, $CDCl_3$, 293 K).

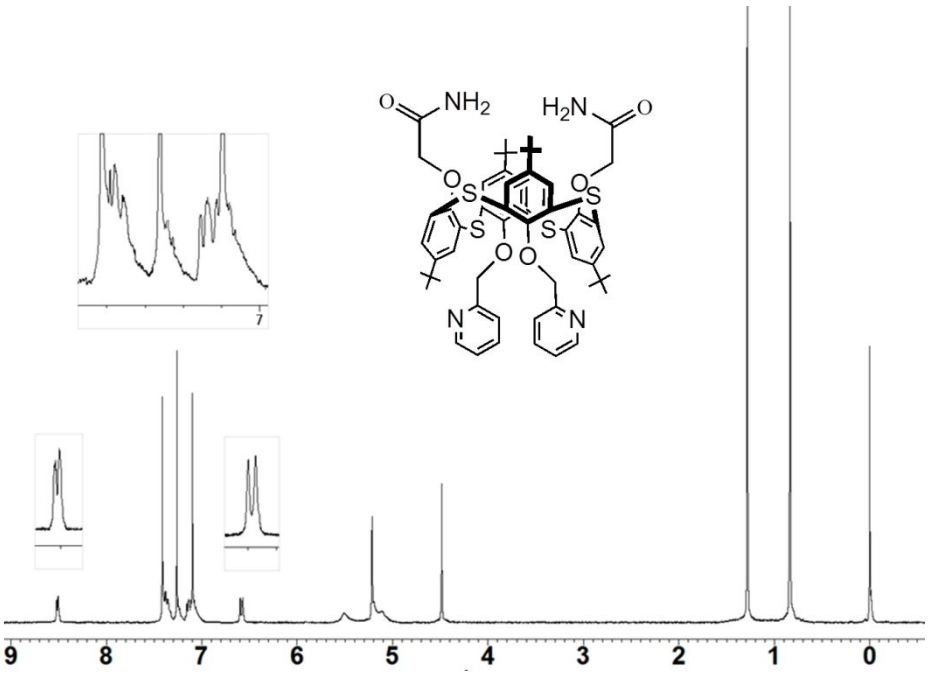


**Figure S3**. $^{1}$H–NMR spectrum of **3** (300 MHz, $CDCl_3$, 293 K).

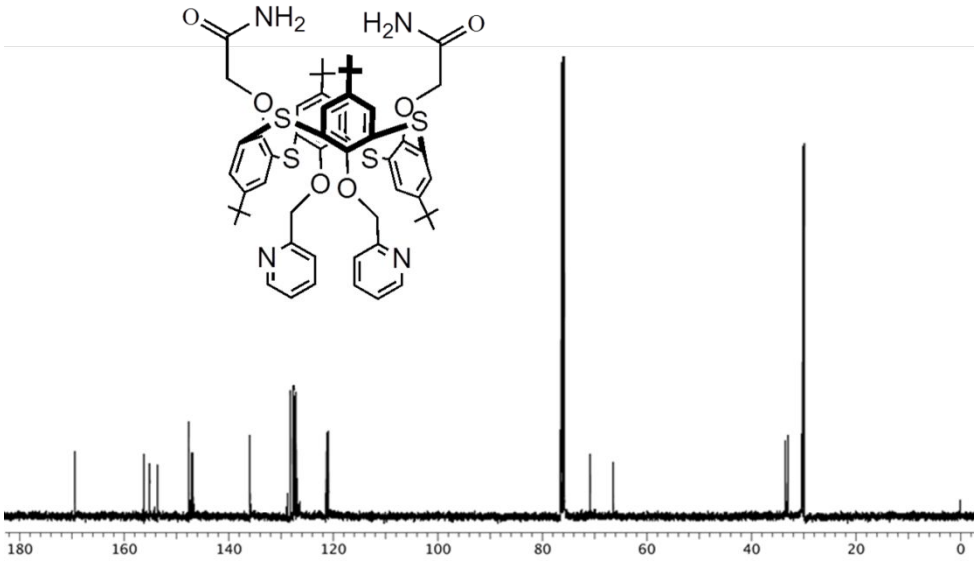


**Figure S4**. $^{13}$C–NMR spectrum of **3** (400 MHz, $CDCl_3$, 293 K).

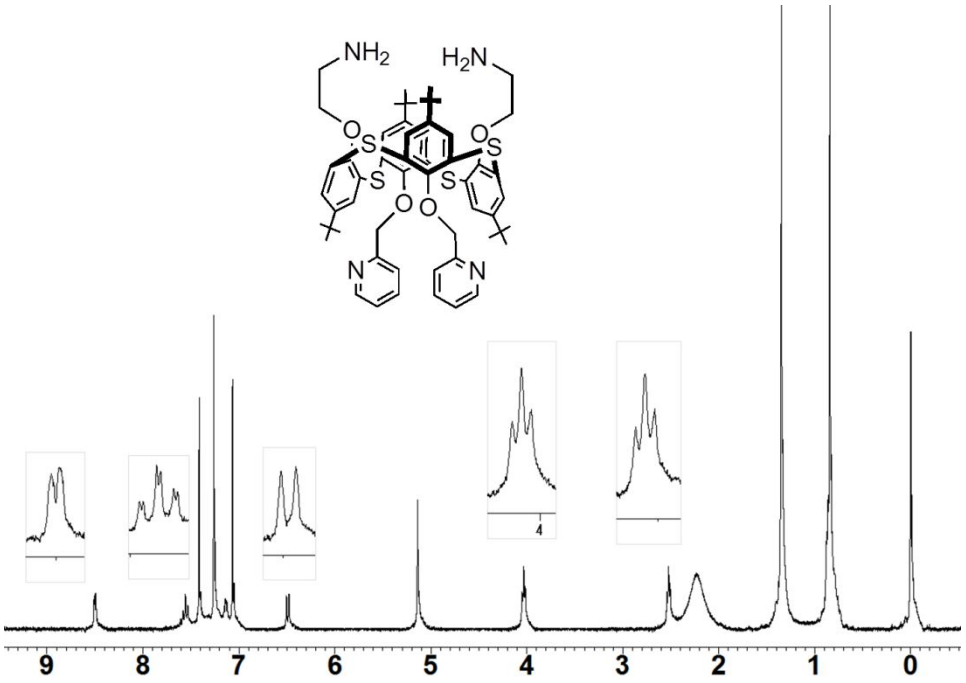


**Figure S5**. $^{1}$H–NMR spectrum of **4** (300 MHz, $CDCl_3$, 293 K).

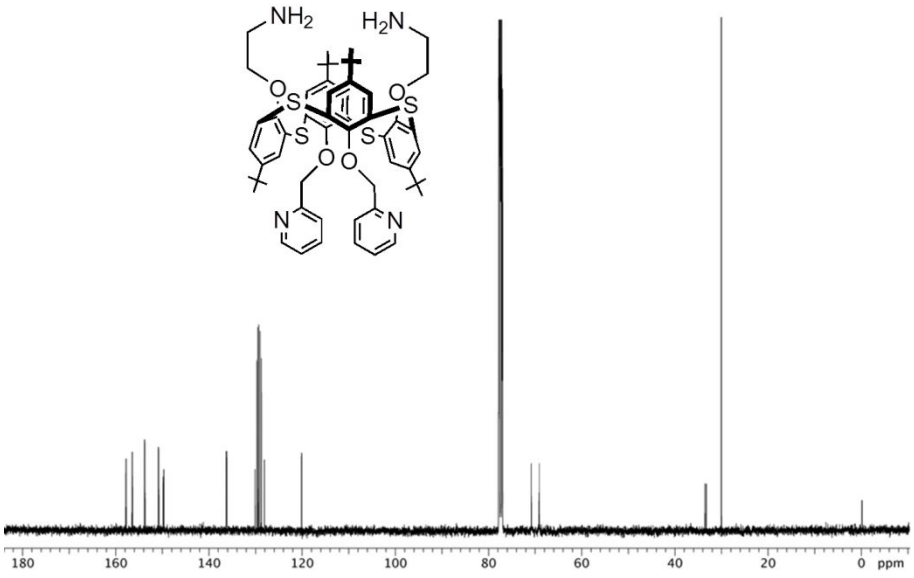


**Figure S6**. $^{1}$H–NMR spectrum of **4** (300 MHz, $CDCl_3$, 293 K).

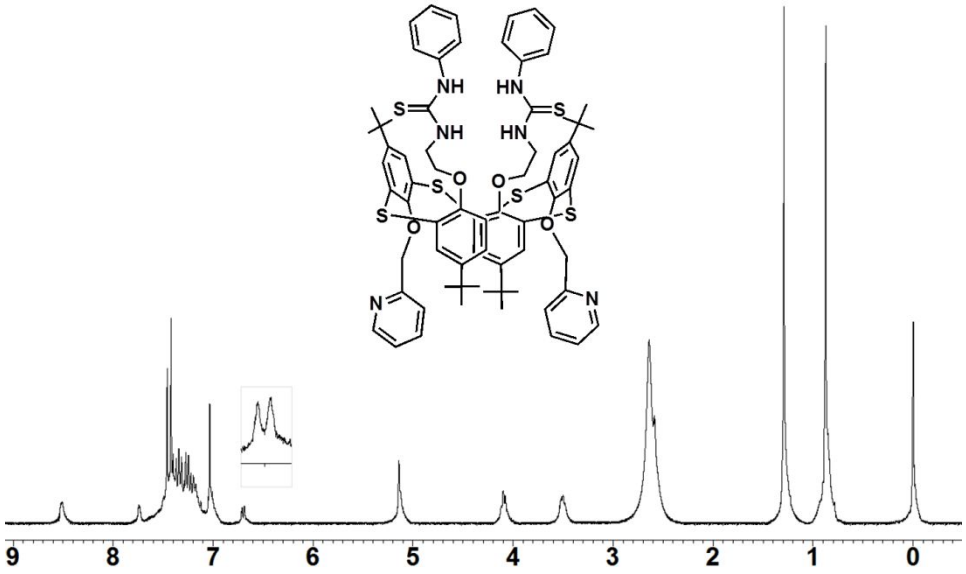


**Figure S7**. $^{1}$H–NMR spectrum of **5a** (400 MHz, $CDCl_3$, 293 K).

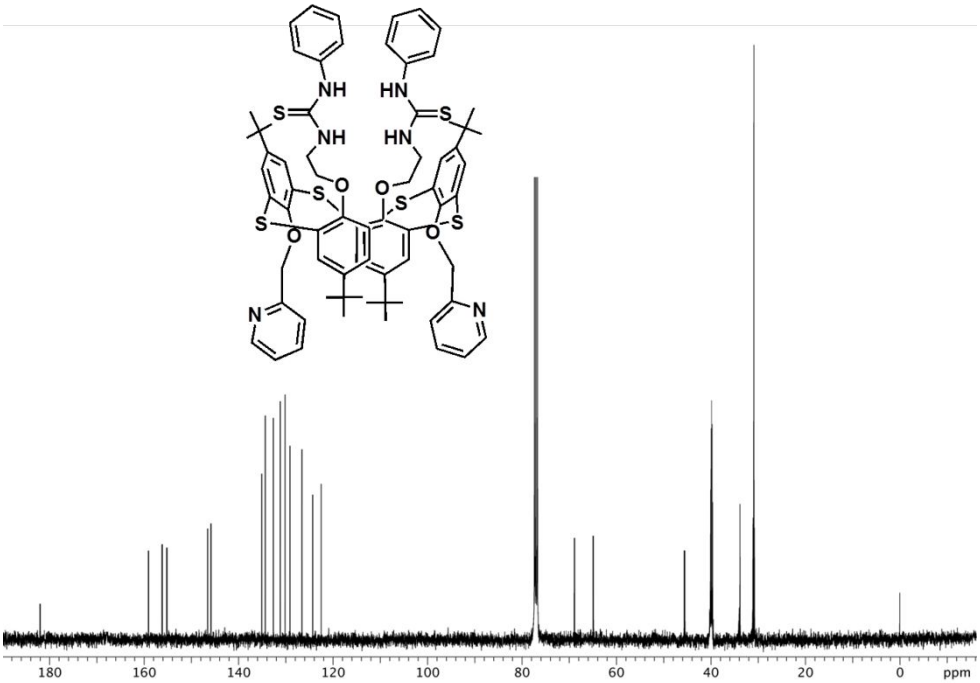


**Figure S8**. $^{13}$C–NMR spectrum of **5a** (300 MHz, $CDCl_3$–DMSO-$d_6$, 293 K).

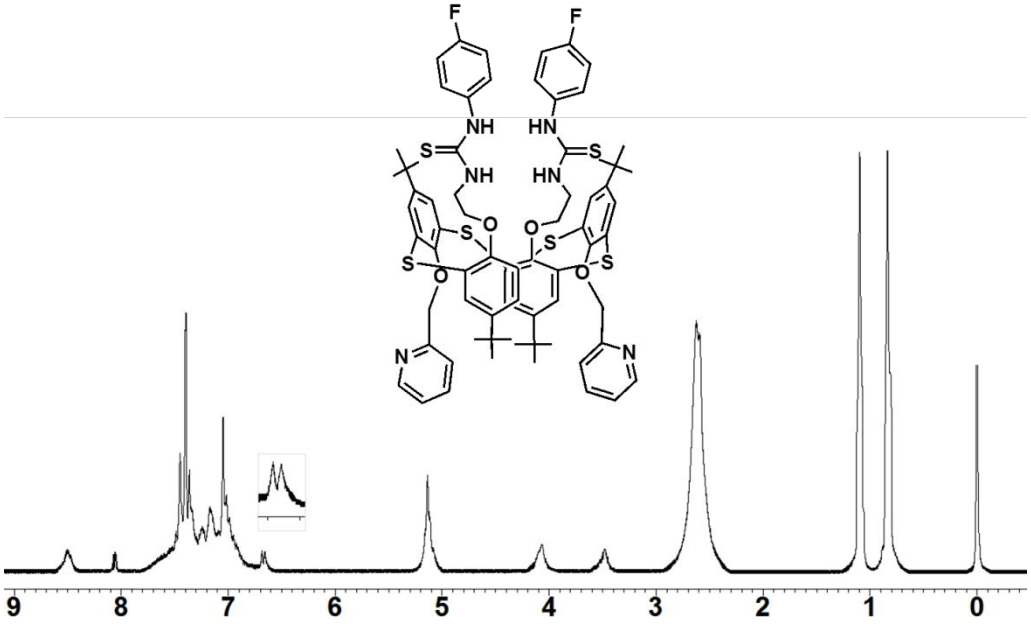


**Figure S9**. $^{1}$H–NMR spectrum of **5b** (400 MHz, $CDCl_3$–DMSO-$d_6$, 293 K).

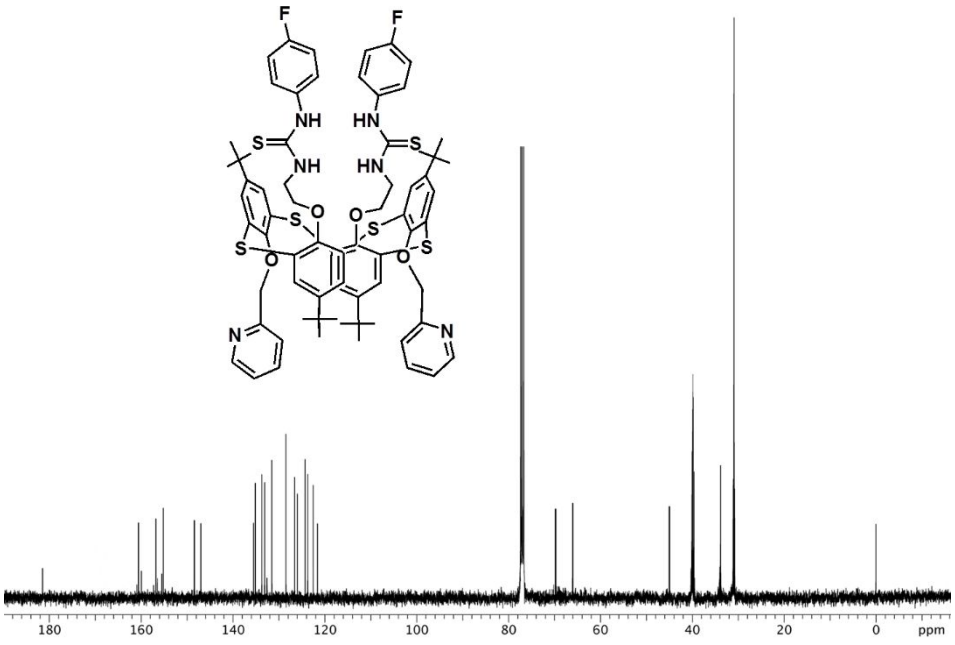


**Figure S10**. $^{13}$C–NMR spectrum of **5b** (300 MHz, $CDCl_3$–DMSO-$d_6$, 293 K).

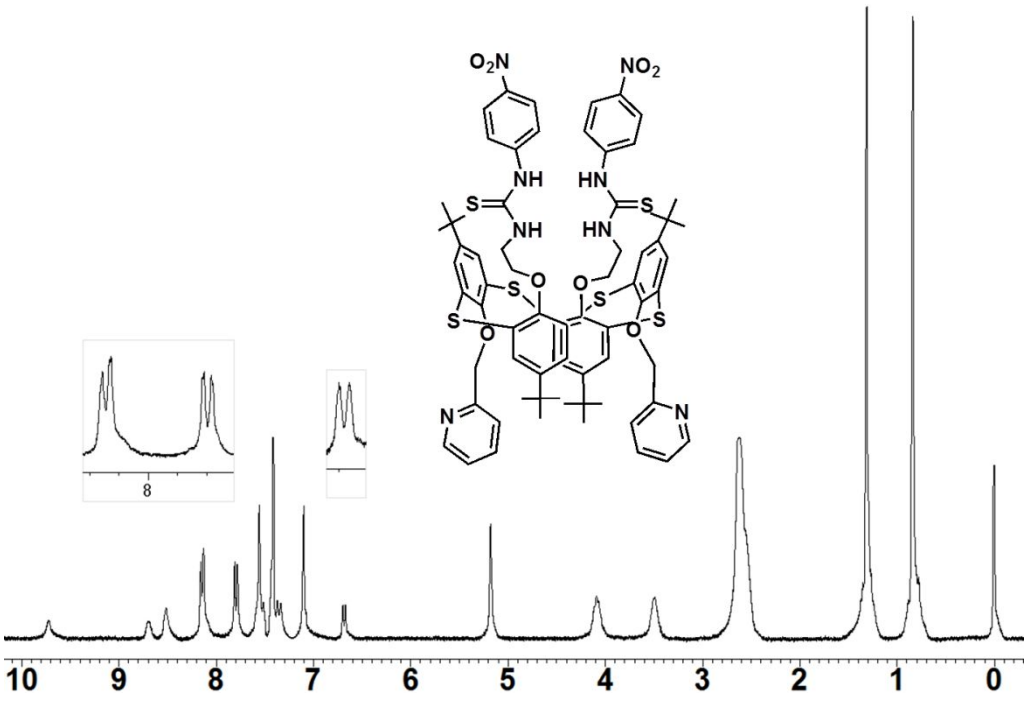


**Figure S11**. $^{1}$H–NMR spectrum of **5c** (400 MHz, $CDCl_3$–DMSO-$d_6$, 293 K).

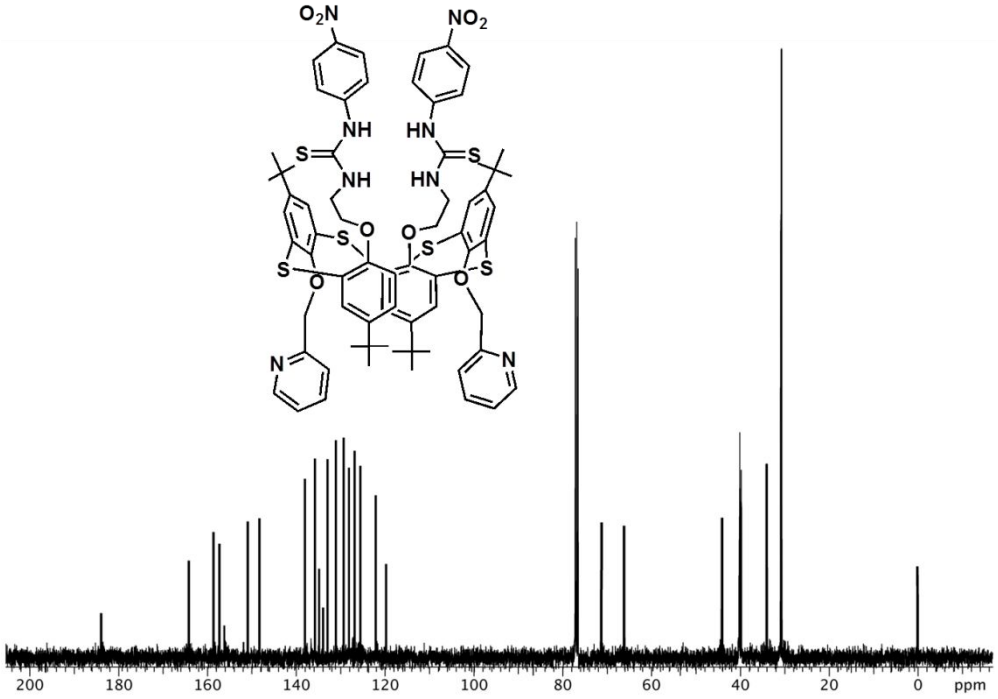


**Figure S12**. $^{13}$C–NMR spectrum of **5c** (300 MHz, $CDCl_3$–DMSO-$d_6$, 293 K).

**X–ray crystal structure of receptor 5a**

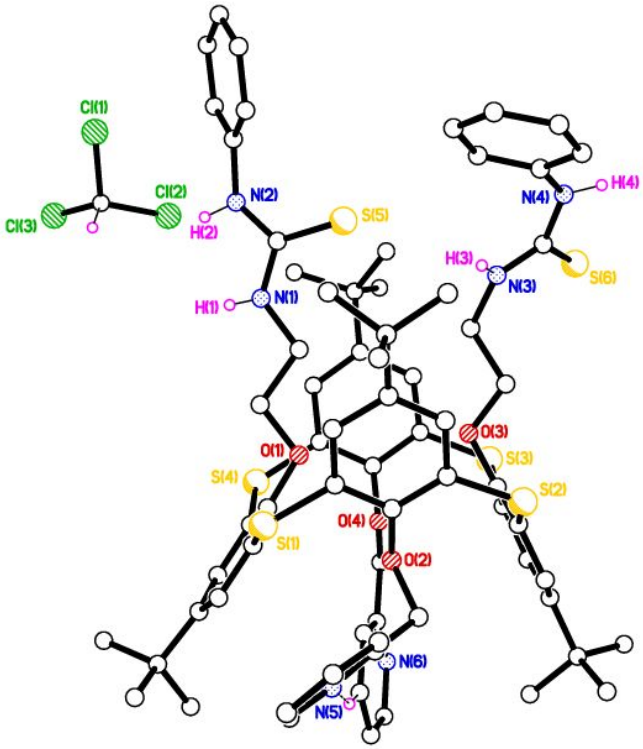


**Figure S13**. The first thiacalixarene in the asymmetric unit with the chloroform solvent of crystallization, showing intramolecular C–H···N hydrogen bonding between opposing pyridine rings. Minor disorder components and H atoms not involved in H-bonding are omitted for clarity.

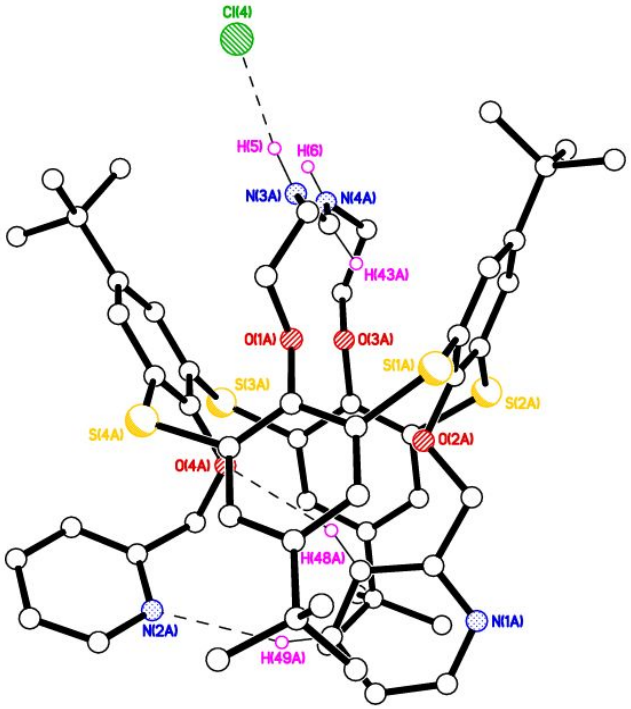


**Figure S14**. The second, modified, thiacalixarene in the asymmetric unit, showing intramolecular hydrogen between opposing pyridine groups and the charge-assisted N–$H^{+}$···$Cl^{-}$ hydrogen bonding at the top of the figure. Most H atoms not involved in H-bonding are omitted for clarity.

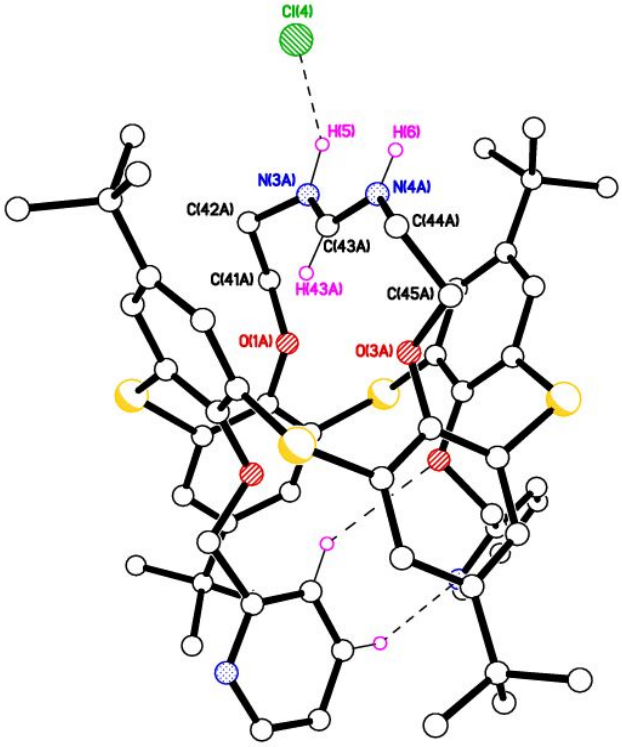


**Figure S15**. Alternative view of the second thiacalixarene in the asymmetric unit, emphasizing the novel functional group at the top of the molecule exhibiting a delocalized positive charge, acting as a counter cation for $Cl^-$ anion capture. H atoms not involved in H-bonding are omitted for clarity.

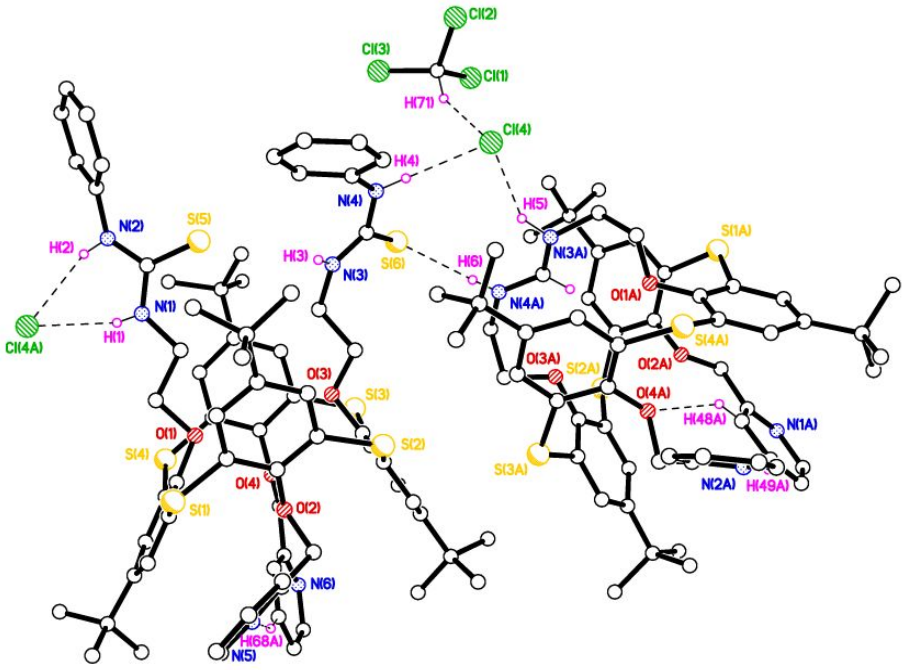


**Figure S16**. The asymmetric unit of **5a**, showing the intermolecular S···H–N hydrogen bonding between the two thiacalixarenes and the N–H···Cl interactions between each thiacalixarene and the $Cl^-$ anion. Minor disorder components and H atoms not involved in H-bonding are omitted for clarity.

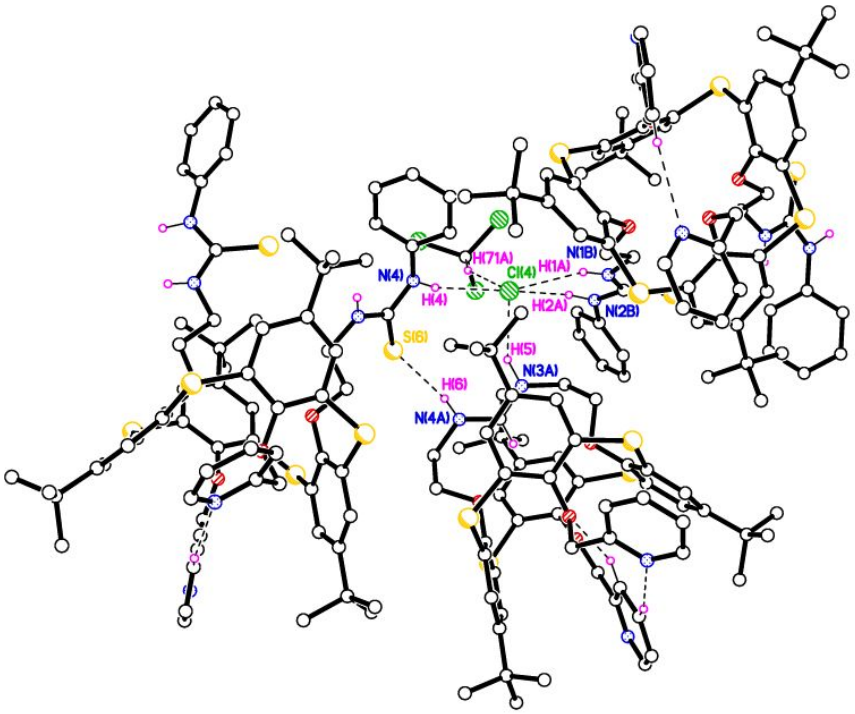


**Figure S17**. X-Ray crystal structure of **5a**, highlighting the capture of the $Cl^-$ anion between three thiacalixarenes via N–H···Cl hydrogen bonding and the (disordered) chloroform solvent of crystallization. Minor disorder components and H atoms not involved in H-bonding are omitted for clarity.

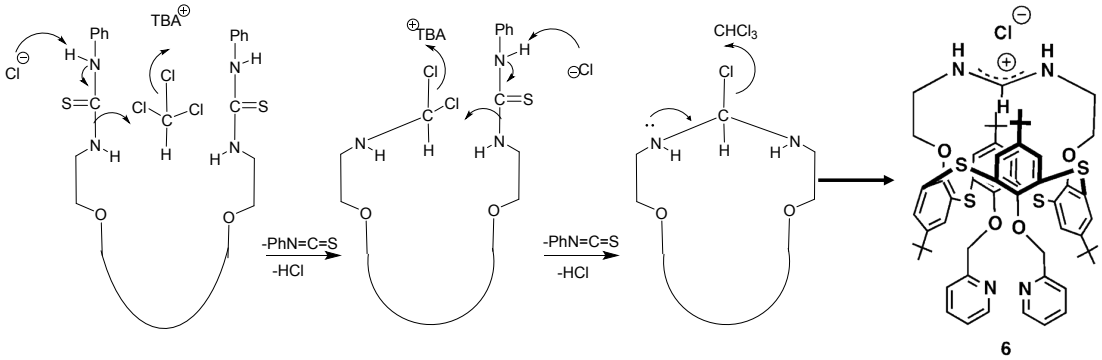


**Scheme S1**. Schematic representation of possible mechanism of the formation of **6** from **5a**.

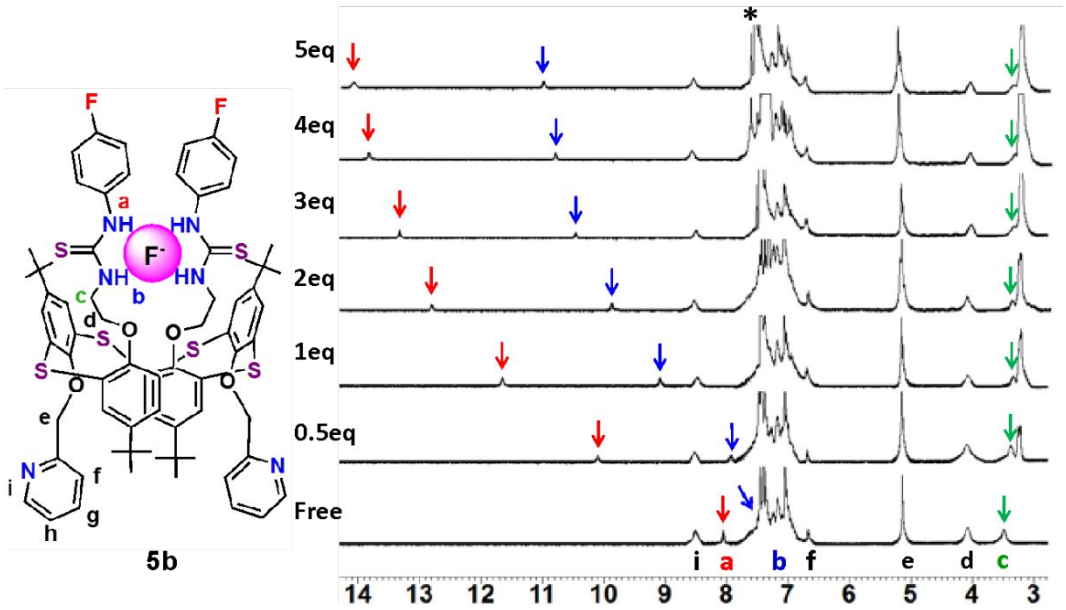


| **5a** (mol$^{-1}$) | **F**$^{-}$ (mol$^{-1}$) | $NH_a$ Proton (ppm) | $NH_b$ Proton (ppm) |
|---|---|---|---|
| 4.00E-03 | 0 | 8.050 | 7.600 |
| 4.00E-03 | 2.00E-03 | 10.090 | 8.420 |
| 4.00E-03 | 4.00E-03 | 11.550 | 9.100 |
| 4.00E-03 | 8.00E-03 | 12.750 | 9.820 |
| 4.00E-03 | 1.20E-02 | 13.300 | 10.415 |
| 4.00E-03 | 1.60E-02 | 13.800 | 10.750 |
| 4.00E-03 | 2.00E-02 | 13.850 | 10.810 |

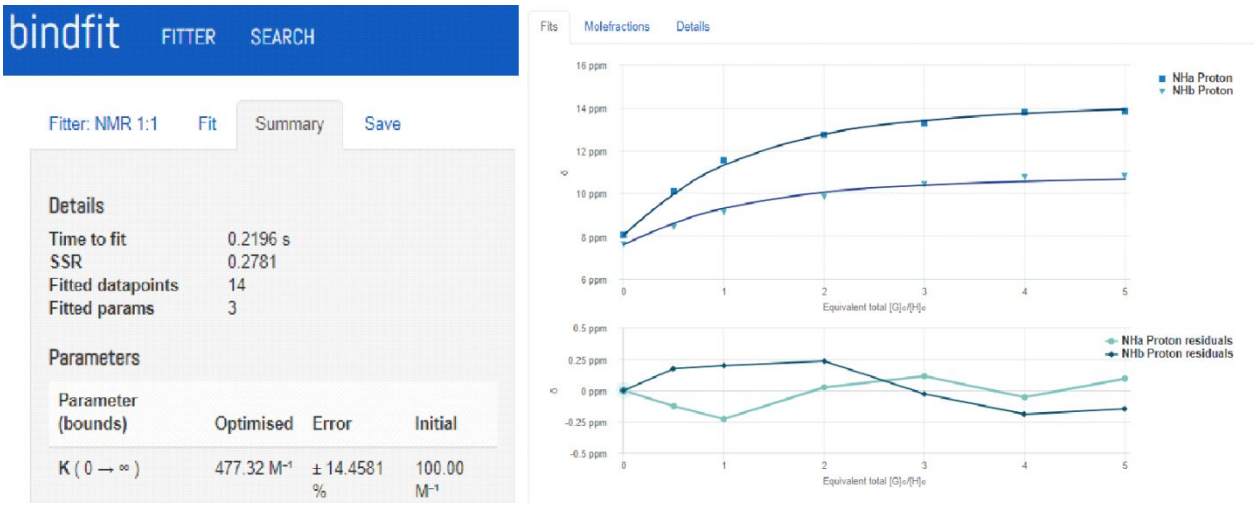


**Figure S18**. $^{1}$H NMR spectroscopic stack plot of a $CDCl_3$–DMSO-$d_6$ (10:1, v/v) solution of **5b** ($4.0 \times 10^{-3}$ M) upon addition of *n*-$Bu_4NF$ in $CD_3CN$. ($K_a = 477 \pm 14$ M$^{-1}$) and the screen capture from the **1:1** global fit analysis using http://supramolecular.org.

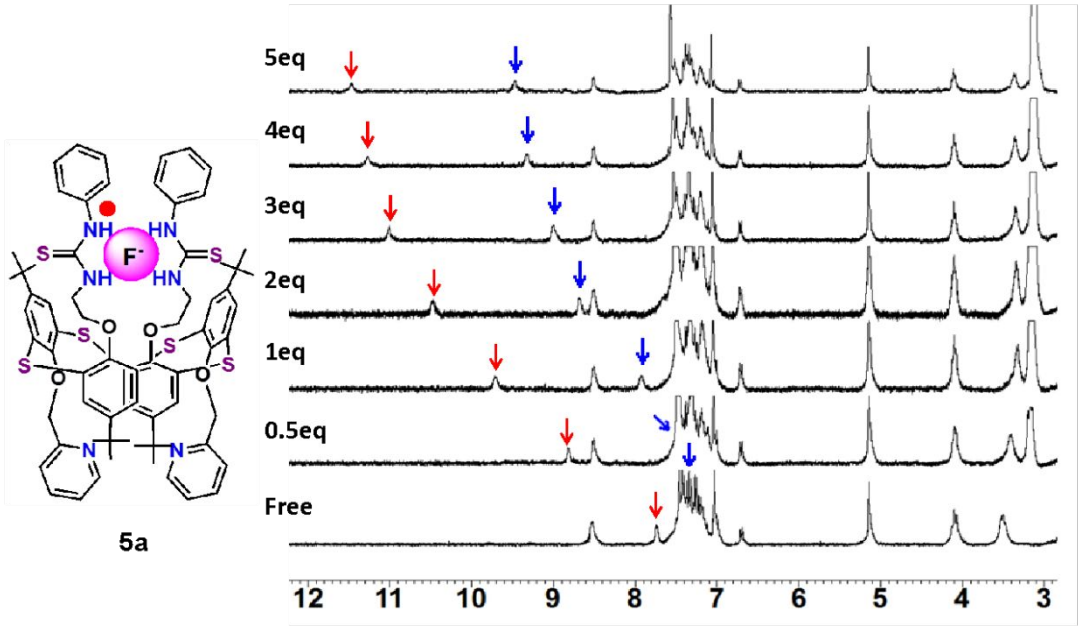


**5a**

| **5a** ($mol^{-1}$) | $F^-$ ($mol^{-1}$) | $NH_a$ Proton (ppm) | $NH_b$ Proton (ppm) |
|---|---|---|---|
| 4.00E-03 | 0 | 7.720 | 7.150 |
| 4.00E-03 | 2.00E-03 | 8.800 | 7.550 |
| 4.00E-03 | 4.00E-03 | 9.700 | 7.900 |
| 4.00E-03 | 8.00E-03 | 10.500 | 8.640 |
| 4.00E-03 | 1.20E-02 | 11.000 | 8.980 |
| 4.00E-03 | 1.60E-02 | 11.250 | 9.340 |
| 4.00E-03 | 2.00E-02 | 11.400 | 9.440 |

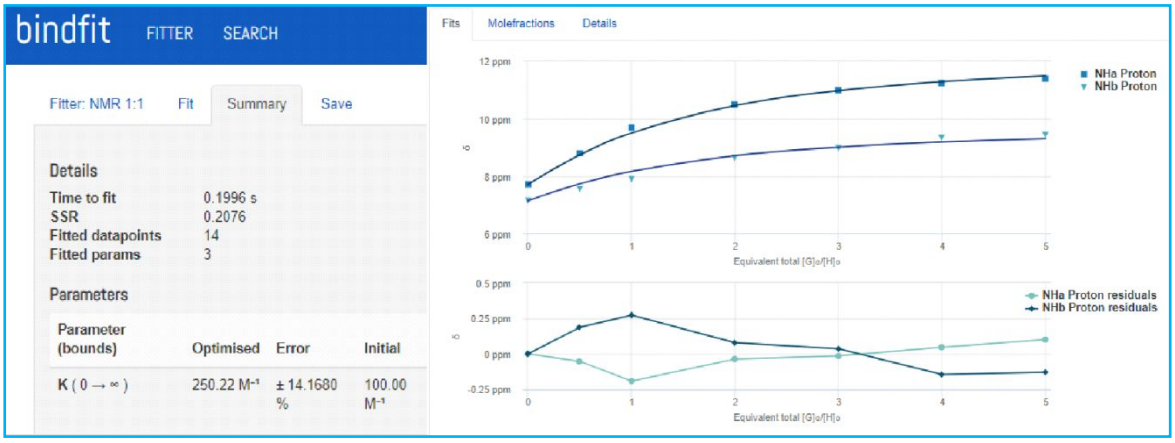


**Figure S19**. $^1$H NMR spectroscopic stack plot of a $CDCl_3$–DMSO-$d_6$ (10:1, v/v) solution of **5a** ($4.0 \times 10^{-3}$ M) upon addition of *n*-$Bu_4NF$ in $CD_3CN$. (($K_a = 250 \pm 14$ $M^{-1}$). and the screen capture from the **1:1** global fit analysis using http://supramolecular.org.

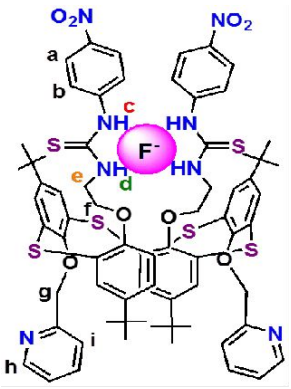


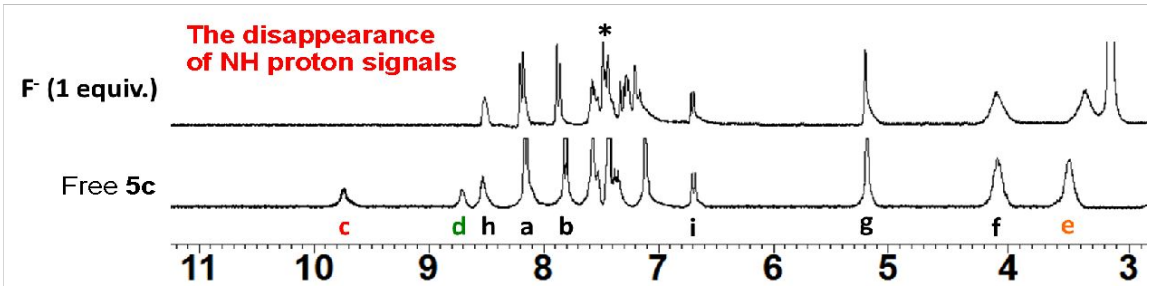


**Figure S20**. $^1$H NMR spectroscopic stack plot of a $CDCl_3$–DMSO-$d_6$ (10:1, v/v) solution of **5c** ($4.0 \times 10^{-3}$ M) upon addition of $Bu_4NF$ in $CD_3CN$.

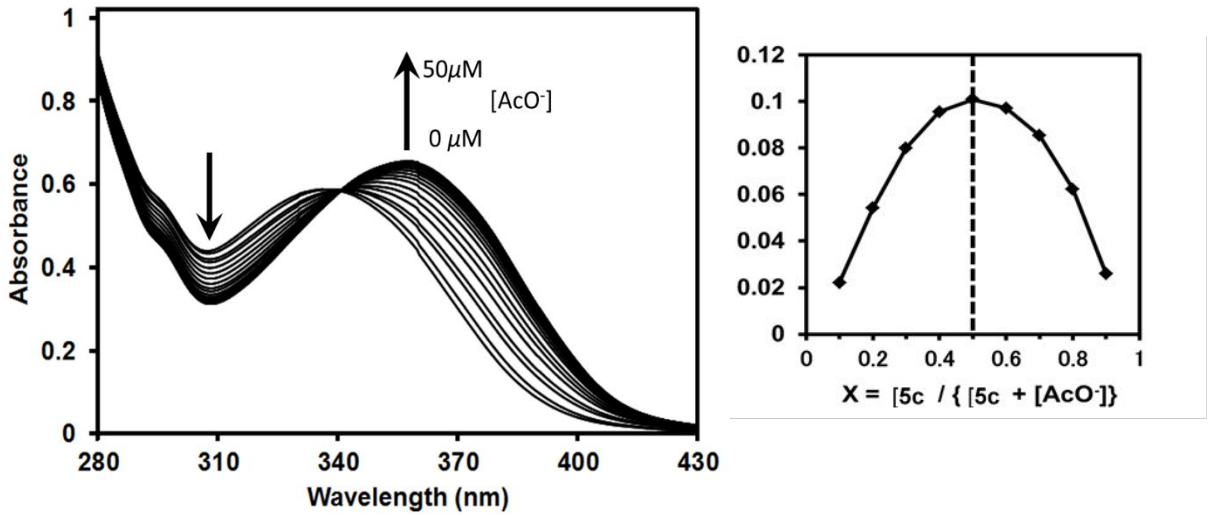


**Figure S21**. *Left*: UV–vis absorption spectra changes of **5c** (2.5 μM) upon the addition of $AcO^-$ ion (0–50 μM) as its tetrabutylammonium salt in $CH_2Cl_2$–DMSO (10:1, v/v) at 298 K. *Right*: Job's plot showing the 1:1 binding of **5c** to $AcO^-$ ion from the UV-vis titration method at 358 nm in $CH_2Cl_2$–DMSO (10:1, v/v).

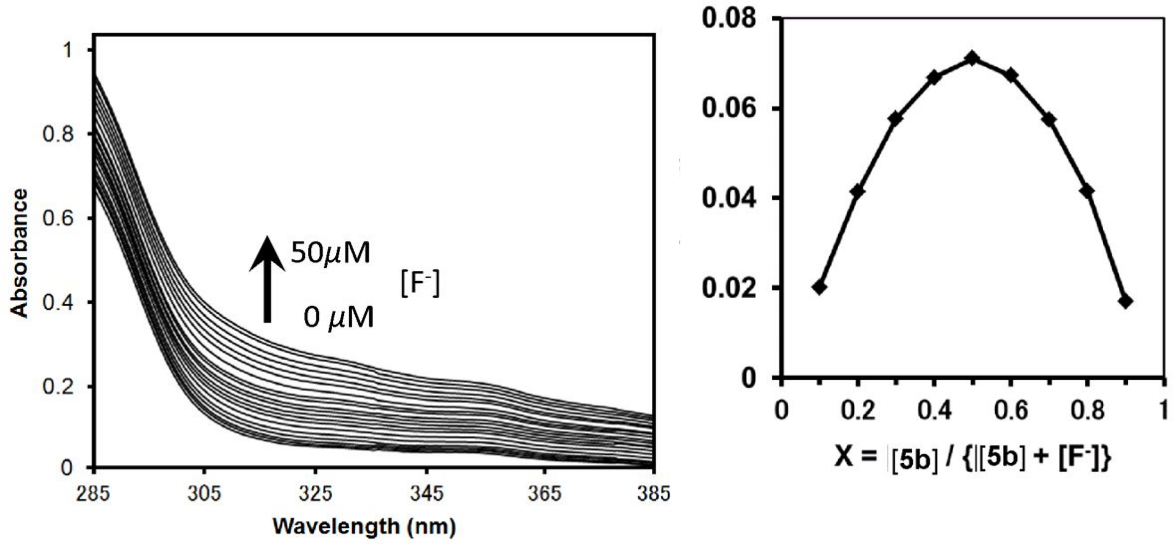


**Figure S22**. *Left*: UV–vis absorption spectra changes of **5b** (2.5 μM) upon the addition of $F^-$ ion (0–50 μM) at 298 K as a $Bu_4NF$ salt in $CH_2Cl_2$–DMSO (10:1, v/v). *Right*: Job's plot showing the 1:1 binding of **5b** to $F^-$ ion from the UV-vis titration method at 358 nm in $CH_2Cl_2$–DMSO (10:1, v/v).

**Table S1**. The DFT interaction energies ΔIE (kJ $mol^{-1}$) calculated from the geometry optimized structure of receptors **L** (*For*: **5a**: R= H; **5b**: R= F; and **5c**: R= $NO_2$**)** and complexes with the anions ($F^-$, $Cl^-$, $AcO^-$, and $H_2PO_4^-$) and cation $Ag^+$ using B3LYP/LANL2DZ basis set in gas phase, dichloromethane (DCM) and dimethyl sulfoxide (DMSO) solvent system using *Gaussian 16*[1] at the B3LYP level of DFT and the LANL2DZ basis set.[2].

| Complex | ΔIE (kJ $mol^{-1}$) in gas phase | | | ΔIE (kJ $mol^{-1}$) in DCM solvent | | | ΔIE (kJ $mol^{-1}$) in DMSO solvent | | |
|---|---|---|---|---|---|---|---|---|---|
| | **5a** (R= H) | **5b** (R= F) | **5c** (R= $NO_2$) | **5a** (R= H) | **5b** (R= F) | **5c** (R= $NO_2$) | **5a** (R= H) | **5b** (R= F) | **5c** (R= $NO_2$) |
| **L**⊃$F^-$ | -484.91 | -505.38 | -551.35 | -242.11 | -249.53 | -274.69 | -206.34 | -225.79 | -231.55 |
| **L**⊃$Cl^-$ | -296.45 | -317.00 | -362.33 | -112.51 | -118.86 | -138.44 | -82.87 | -101.32 | -100.61 |
| **L**⊃$AcO^-$ | -294.52 | -314.05 | -361.34 | -125.67 | -132.34 | -155.99 | -95.96 | -115.25 | -104.33 |
| **L**⊃$H_2PO_4^-$ | -268.66 | -289.58 | -339.47 | -119.77 | -126.41 | -136.37 | -91.63 | -105.16 | -101.83 |
| **L**⊃$Ag^+$ | -440.17 | -436.59 | -436.38 | – | – | – | v | – | – |
| **L**⊃$Ag^+$ | – | -435.64 | – | – | -169.28 | – | – | -146.90 | – |
| $Ag^+$⊂**L**⊃$F^-$ | – | -1090.11 | – | v | -417.73 | – | v | -364.91 | – |

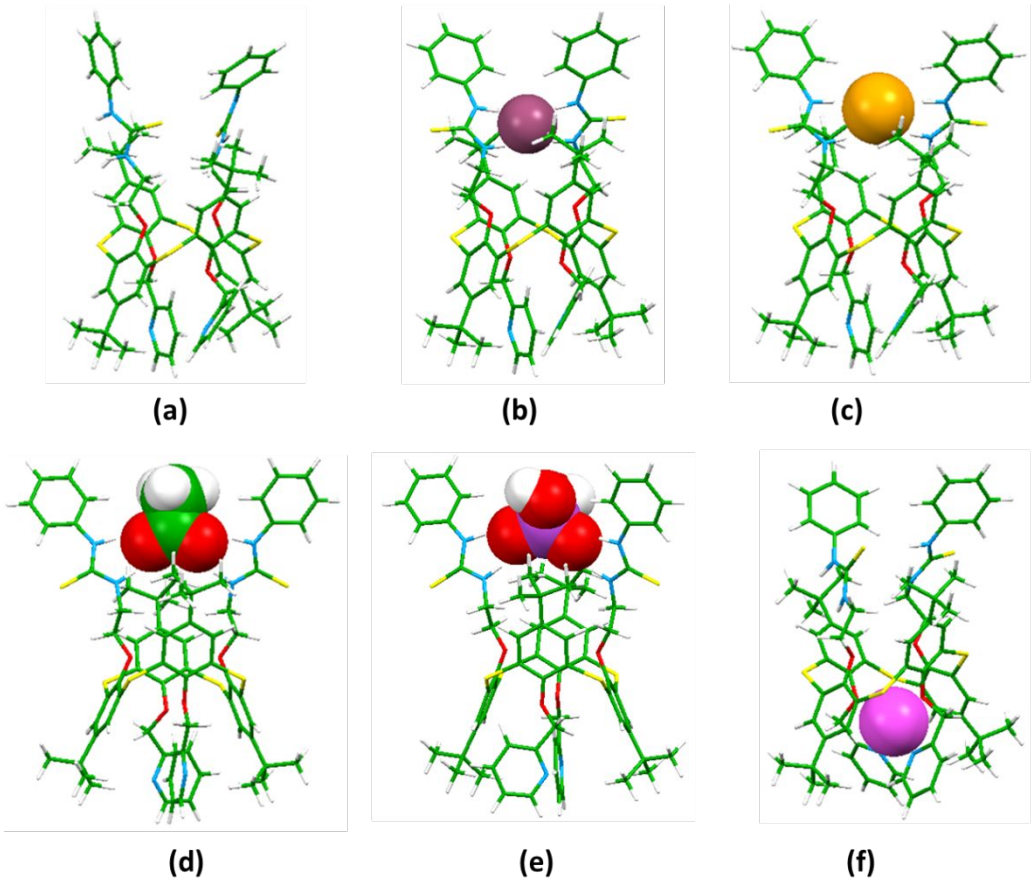


**Figure S23**. Geometry-optimized (PBE0/LANL2DZ) structures of receptor **5a** (R= H) and complexes with the anions (b-e) ($F^-$, $Cl^-$, $AcO^-$, and $H_2PO_4^-$) and $Ag^+$(f) ion by using B3LYP/LANL2DZ basis set in gas phase. Colour code: carbon atoms = green, oxygen atoms = red, nitrogen atoms = blue, and $Ag^+$ = magenta. $F^-$ = purple; $Cl^-$ = orange; Hydrogen atoms = white; phosphorus atom= light purple.

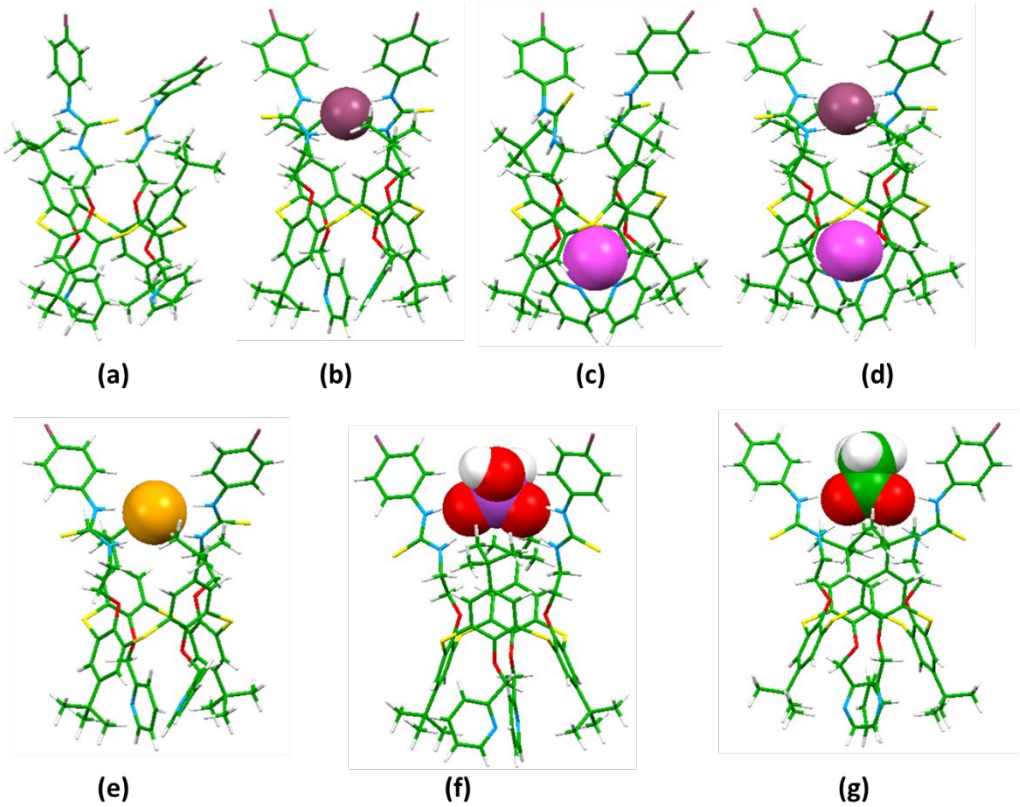


**Figure S24**. Geometry-optimized (PBE0/LANL2DZ) structures of receptor **5b** (R= F) and complexes with the anions ($F^-$, $Cl^-$, $AcO^-$, and $H_2PO_4^-$), $Ag^+$ ion (c) and $Cl^-$ in presence of $Ag^+$ ion (d) by using B3LYP/LANL2DZ basis set in gas phase. Colour code: carbon atoms = green, oxygen atoms = red, nitrogen atoms = blue, and $Ag^+$ = magenta. $F^-$ = purple; $Cl^-$ = orange; Hydrogen atoms = white; phosphorus atom= light purple.

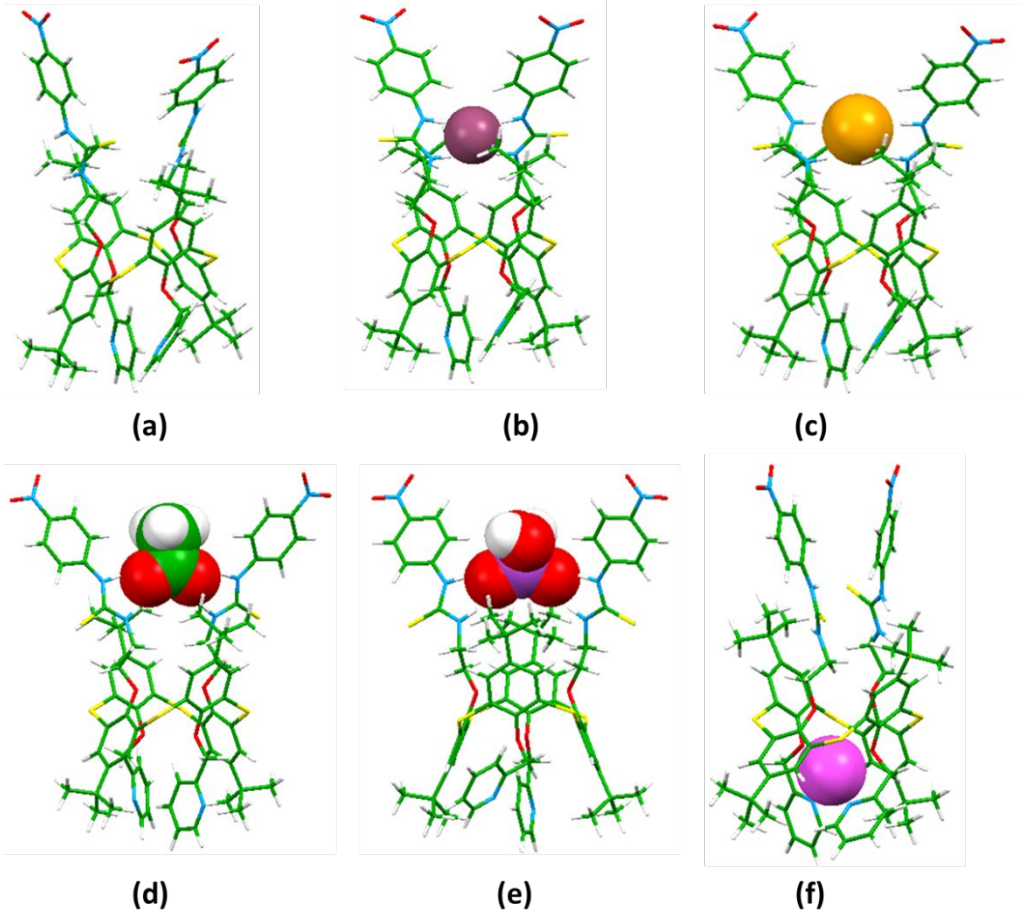


**Figure S25**. Geometry-optimized (PBE0/LANL2DZ) structures of receptor **5c** (R= $NO_2$) and complexes with the anions ($F^-$, $Cl^-$, $AcO^-$, and $H_2PO_4^-$) and $Ag^+$ ion by using B3LYP/LANL2DZ basis set in gas phase. Colour code: carbon atoms = green, oxygen atoms = red, nitrogen atoms = blue, and $Ag^+$ = magenta. $F^-$ = purple; $Cl^-$ = orange; Hydrogen atoms = white; phosphorus atom= light purple.

**References:**

1. M. J. Frisch, *et al*., *Gaussian 16*, Revision C.01 Gaussian, Inc., Wallingford CT, 2019.
2. (a) J. P. Perdew, K. Burke, M. Ernzerhof, Generalized Gradient Approximation Made Simple. *Phys. Rev. Lett.* 1996, **77**, 3865; (b) J. P. Perdew, K. Burke, M. Ernzerhof, Generalized Gradient Approximation Made Simple. *Phys. Rev. Lett.* 1997, **78**, 1396.